INTERFEROMETRIC STUDY OF NATURAL CONVECTION FROM AN INCLINED FLAT PLATE FACING DOWNWARDS

A Thesis Submitted
in partial Fulfilment of the Requirements
for the Degree of
MASTER OF TECHNOLOGY

By
YASH PAUL GUPTA

to the

DEPARTMENT OF MECHANICAL ENGINEERING

INDIAN INSTITUTE OF TECHNOLOGY KANPUR

AUGUST, 1975

CERTIFICATE

This is to certify that this work on "Interferometric Study of Natural Convection From an Inclined Flat Plate Facing Downwards" has been carried out under my supervision and has not been submitted elsewhere for a degree.

P.N. KAUL
Assistant Professor
Department of Mechanical Engineering
Indian Institute of Technology, Kanpur

ACKNOWLEDGEMENTS

The author expresses his deep sense of gratitude to Professor P.N. Kaul for his invaluable guidance in the initiation, progress and completion of the present study.

The author is grateful to Dr. V.K. Garg for useful discussions and various suggestions made during the course of this work.

The author also wishes to put on record his gratefulness to

Shri S.K. Chaturvedi for willing assistance and invaluable advice during the conduct of the experiment,

Shri Shambhu Nath Sharma for his help in fabrication and setting up the experimental set-up,

Shri D.K. Sarkar for his help in photography of the fringe patterns.

Last but not the least, the author appreciates the excellent typing of Shri D.P. Saini.

Y.P. Gupta

CONTENTS

LIST OF FIGURES

NOMENCLATURE

c_x	Local correlation coefficient.
c	Average correlation coefficient.
c°	Degree centigrade.
C	Velocity of light, m/sec.
C_{va}	Velocity of light in vacuum, m/sec.
F°	Degree Fahrenheit.
g	Gravitational acceleration, cm/sec^2.
h	Average heat transfer coefficient, $Kcal/hr-cm^2-c°$
h_x	Local heat transfer coefficient, $Kcal/hr-cm^2-c°$
K	Thermal conductivity of air, Kcal/hr-cm-c°.
K°	Degree Kelvin.
l	Length of heated path of light, mm.
L	Width of plate, mm.
n	Refractive index of air.
n_a	Refractive index of air at room temperature.
$\triangle N$	Fringe shift.
q_w	Convective heat flux at the plate surface, $Kcal/hr-cm^2$.
R_t	Resistance of platinum thermometer at temperature t.
R_o	Resistance of platinum thermometer at ice point.
S	Distance from plate surface, mm.

T	Temperature of air infront of the plate surface, K°.
T_a	Temperature of ambient air, K°.
t_w	Temperature at the wall of the plate, c°.
t_a	Temperature of ambient air, c°.
t_f	Mean film temperature, c°.
x	Distance from the leading edge of the plate, cm.
k'	Dimensionless constant for air.
k''	Dimensionless constant characteristic of air.
Gr	Grashof number $\frac{g L^3 \beta (t_w - t_a)}{\nu^2}$
Pr	Prandtl number $(\frac{\mu c_p}{K})$
Nu	Nusselt number (h L/K).
R_a	Rayleigh number (Gr. Pr.).
ρ	Density of air, (Kg/m^3)
ρ_a	Density of air at room temperature, (Kg/m^3).
β	Coefficient of thermal expansion, $K^{\circ -1}$
λ_o	Wave length of light in vacuum, mm.
ν	Kinematic viscosity, $(cm^2/sec.)$.
θ	Inclination of the plate with the vertical, degrees.
α	Fundamental coefficient of coil.

ABSTRACT

Interferometric Study of Natural Convection from
an Inclined Flat Plate Facing Downwards
Yash Paul Gupta
Master of Technology
Department of Mechanical Engineering
Indian Institute of Technology, Kanpur
August 1975

Natural convection from an electrically heated inclined flat plate (120 x 60 x 6 mm) facing downwards has been studied by using interferometry. The plate with unrestricted edges open to flow from all sides has been tested along its longish axis. Temperature distribution for the plate surface has been calculated from the fringe shifts measured on the interferogram (fringe pattern). Heat transfer due to convection to the surroundings has been determined from the temperature gradients at the plate surface. It is proposed that natural convection heat transfer from an inclined flat plate facing downwards can be correlated by the formula :

$$Nu = 0.626\ (Gr.\ Pr.\ Cos\theta)^{\frac{1}{4}}$$

Heat transfer coefficients yielded by the above correlation are, however, 6.6% higher than those reported in the literature for the vertical plate.

The study also includes the use of Schlieren apparatus for flow visualization purposes. The Schlieren photograph for the horizontally heated flat plate shows that the flow is symmetrical about the middle of the plate. The boundary layer is seen to be maximum near the center of the plate and reduces gradually to the minimum around the free edges. The boundary layer is not zero at the free edges as postulated by the previous researchers in their theoretical analyses given in the literature. Therefore, the heat transfer from a horizontal flat plate facing downwards can not be determined by treating it as a limiting case of the inclined flat plate facing downwards.

CHAPTER 1

1.1 INTRODUCTION:

Free or natural convection is the mode of heat transfer that occurs when a body is placed in a fluid at a temperature different from that of the body. As a result of the temperature difference, density changes occur in the fluid around the body. The fluid starts to flow due to the buoyancy forces created by density gradients in the fluid. However, in the forced convection heat transfer, the fluid flow is imposed and maintained mechanically, either by a pump or a compressor or a blower.

Heat transfer due to free convection plays an important role in many practical engineering applications. Heat losses occur from pipes carrying heated fluids, walls and ceilings of buildings, steam radiators, evaporators, condensers and other bodies placed in quiescent atmosphere due to free convection. Also cooling of structural parts in propulsion systems like gas turbine blades, rocket nozzles and combustion chamber walls is achieved by free convection flows which are produced by centrifugal forces.

Mathematically speaking, Grashof and Prandtl numbers are the two important non-dimensional parameters which characterise the type of flow in natural convection, while in forced convection, Reynolds number plays

a dominant role. Differential equations for velocity and thermal boundary layers are coupled and consequently an interaction exists between the temperature and the velocity fields, making the problem of natural convection analytically more complicated than that of forced convection. Moreover, if there exist large temperature gradients within the fluid, variations of properties other than density, like thermal conductivity and viscosity, should be taken into account to make an appropriate analytical study of the flow. Hence, both the momentum and energy equations have to be solved simultaneously in any study of natural convection problem, and their solutions are tedious and complicated, if not impossible.

Many natural convection phenomena are therefore, investigated experimentally to avoid the difficulties inherent in obtaining an analytical solution and also to check the validity of analytical solutions wherever available.

1.2 REVIEW OF PREVIOUS WORK:

A simplified model of many free convection problems was investigated theoretically as well as experimentally by Schmidt and Beckman [1], who studied the free convection flow of air on a short vertical hot plate. The agreement between the two (theoretical and experimental) results was seen to be good and the velocity and the thermal boundary layer thicknesses were found to be proportional to $x^{1/4}$, where x is the distance from the leading edge of the plate. Eckert and Jackson [2], found by experiments

on heated vertical flat plates and cylinders that the flow is laminar for Rayleigh number less than 10^8 and turbulent for Rayleigh number greater than 10^{10}. Eckert and Soehnghen [3] used an interferometer to study the mechanism of natural convection heat transfer from a heated vertical aluminum plate to air. It was found that the flow was laminar for the first 20 inches from the bottom; then the transition from laminar to turbulent flow starts at 21 inches at a critical value of the Grashof number of 4×10^8 and a fully developed turbulence occurs near the top of the plate at Grashof number of 3.8×10^{11}. The analysis of laminar free convection flow over a flat plate was extended by Ostrach [4] to include very large Grashof and Prandtl numbers. He found that the velocities and Nusselt numbers of the order of the magnitude of those encountered in forced convection flows could be obtained in free convection flows created by centrifugal force fields. Other experimental investigations include heat transfer in vertical tubes at large Grashof numbers (10^8 to 10^{13}) by Eckert and Diagvilla [5] and natural convection between parallel plates by Lietzke [6], who found that the flow became unsteady at the top of the plate for the value of $Gr\ Pr \simeq 2 \times 10^9$. The mechanism of heat loss due to convection from vertical surfaces was also studied by Griffiths and Davis [7] and they found that, on the whole, convective cooling was proportional to 5/4 power of the temperature excess over surrounding air.

Natural convection from the downward facing horizontal plate has also been studied extensively. Levy [8] treated the case of the horizontal

plate of finite area by means of an approximate analysis based on assumed velocity and temperature profiles in the boundary layer, using the integrated momentum and energy equations for the boundary layer. Wagner [9] applied the integral method of Levy and carried out in detail the calculations of heat transfer from a downward facing heated strip of finite width. He assumed the velocity and temperature layers to be of the same thickness and decrease from a maximum thickness at the center of the strip to zero at the free edge. The results show the Nusselt number to be proportional to the $\frac{1}{5}$ th. power of the product of Grashof and Prandtl number. Stewartson [10] assumed the edges as stagnation points similar to inclined plates, and fluid flow from the edge towards the center. Kadambi [11] and later Kadambi and Drake [12] attempted similar boundary layer analysis for the axisymmetrical case of a circular hot plate facing downward. Singh, Birkebak and Drake [13] have presented solutions for the flow from the center towards the edge using the condition that the boundary layer has zero thickness at the edge. Clifton and Chapman [14] performed an analysis for a two-dimensional plate by setting the boundary layer at the edge equal to a critical depth predicted by analogy to open channel hydraulics. The validity of these approximate solutions depends on the boundary conditions at the plate edge and the velocity and temperature profiles assumed in the respective analyses.

Recently, Aihara et. al. [15] investigated the laminar free convection along the downward - facing surface of an isothermal horizontal

plate and explored the applicable range of boundary layer approximation. Their results closely agreed with the predictions of [13] near the center of the plate. The plate was heated on both sides and on the edge, causing a higher heat flux near the edge. Therefore, the measured heat transfer coefficient close to the edge, was much higher than the prediction of [13]. Aihara et.al. carried the velocity measurements outside the thermal boundary layer and found an appreciable horizontal flow from the edges towards the center. Francisco and Glicksman [16] studied the effect of edge condition on natural convection from a horizontal plate facing downward. A square copper plate (7 x 7 x 1 inch) was used for the heated surface. The plate was thick so as to assure temperature uniformity over the hot surface. The edge conditions studied were as follows:

(i) insulated edges

(ii) bare edges

(iii) cooled to a temperature close to ambient.

It was found that the conditions at the outer edge of a heated horizontal plate facing downward has a marked influence on the thermal boundary layer shape and the heat flux distribution over the entire heated area.

Interest in natural convection on inclined surfaces arose out of attempts to describe thermal stratification in insulated cryogenic propellant vessels, where a substantial portion of heat input occurs in the vessel bottom. Rich [17] made both local heat transfer and boundary layer temperature measurements in the laminar regime on an inclined plate facing

upward. An aluminum plate 4" wide 16" long and 1/8" thick was heated through the use of an electrofilm resistance heating element applied on one side of the plate. On the other side of the plate where the free convection was to be studied, four chromel - alumel thermocouples were spot welded at 3, 6, 10 and 13 inches measured from the bottom of the plate. No constant voltage transformer was used. The test was run in an air-conditioned room, so that the ambient temperature could be maintained constant. Angles of inclination ranged from 0 to 40 degree measured from the vertical. The local heat transfer correlated well with vertical plate data taking the gravitational term in the Grashof number as the gravity component parallel to the surface of the plate.

Investigation of the plate surface temperature distribution shows that the heated surface in [17] is not isothermal. Further, in the absence of a stabilized power supply, the test surface can not be one of a constant heat flux. Also the air conditioner must have disturbed the flow.

Vliet [18] made experimental studies of local heat transfer coefficient on constant heat flux inclined surface facing upward. The plate was 4 ft. high x 3 ft. wide with an electrically heated 2 - mil thick stainless steel sheet insulated on the back. The plate was immersed in a water tank as shown in Fig. 1.2.1. To have a constant leading edge condition, a right angle geometry was maintained near the plate leading edge by attaching a wall perpendicular to the plate, 2 inches below the start of the

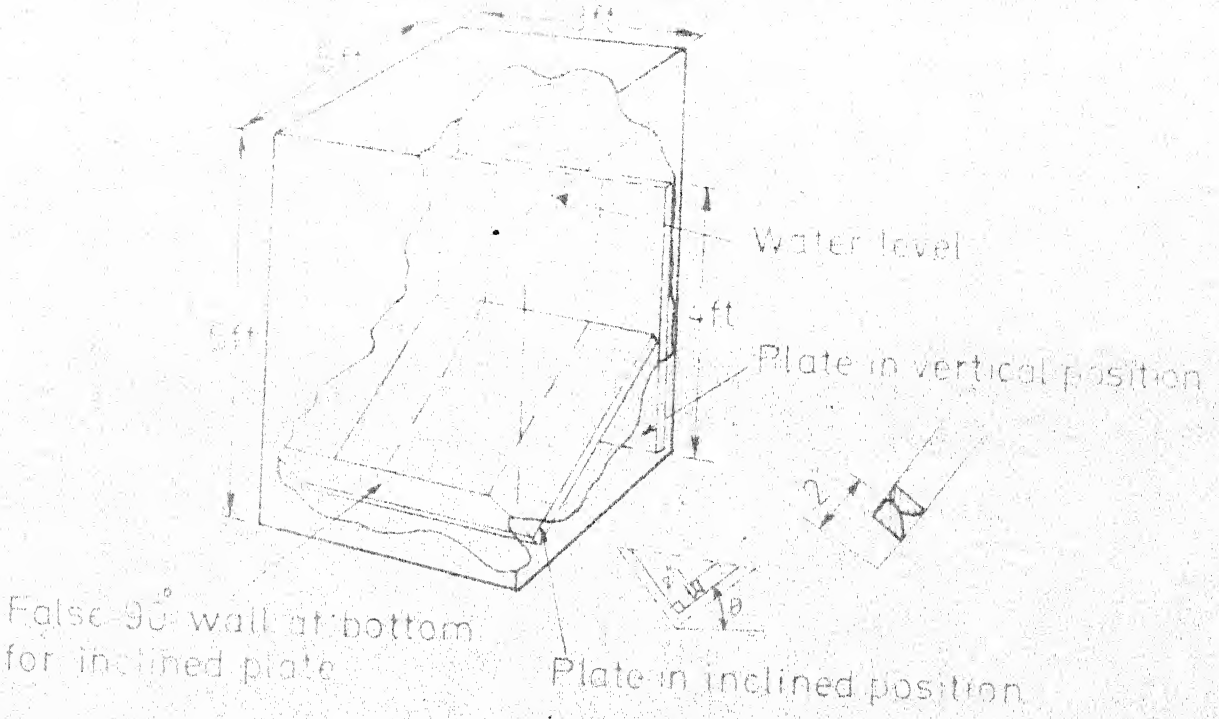

FIG. 2.1 NATURAL CONVECTION TEST APPARATUS FOR INCLINED SURFACE USED BY VLIET [18]

heated section. Experiments were carried with the plate inclined at angles of 30 - 85 degrees with the horizontal. According to the author, there was great uncertainty in the water bath temperature.

Though the leading edge condition was maintained constant, yet the experimental results can not be applied to a more general case with open edges of the plate surface. The right angle geometry will produce its own convection field and its interaction with the convection field of the inclined plate near its leading edge is bound to affect the flow pattern and hence the heat transfer.

1.3 SCOPE OF THE PRESENT WORK:

A detailed consideration of the above referenced literature leads one to the conclusion that not only have the authors used different flow models but also some of the models as in [9], [10], [11] and [12] can not be justified physically. The velocity and temperature boundary layer are of the same thickness only when Prandtl number is unity. For a heated plate facing downward, the boundary layer at the edge can not be assumed as stagnation points similar to inclined plates. The experimental results of Aihara et. al. seem to be more convincing but need to be verified by better methods of measurement.

Accurate experimental results for heat transfer from downward facing hot plate are quite difficult to obtain because of the very low value of the heat transfer coefficient. Heat losses through the walls and

the plate supporting structure can be of the same order of magnitude as the heat transferred to the plate. At low plate temperatures, radiation absorbed from the surroundings is important. When the plate temperature is elevated, radiation emitted by the plate becomes important relative to convection heat loss. Therefore, it is difficult to accurately determine the net convective heat flux from the test plate by a heat balance.

The present work deals with the experimental determination of natural convection heat transfer from an inclined plate facing downward by using optical method, namely interferometry. Compared with other measurement methods in the area of heat transfer, optical methods possess considerable advantages. The measurements do not disturb the temperature field and there are practically no inertial errors in the optical methods so that rapidly changing processes can be accurately followed. This advantage arises from the possibility of recording the entire temperature field on a single photograph.

Test plate of good heat conducting material, aluminum, was heated by a main heater made from nichrome strip (38 SWG) wound around a thin mica sheet. A guard heater was also made in the similar manner to restrict the backward flow of heat. In addition to determining the heat transfer from an inclined plate facing downward, the present work could also serve as a check for the heat transfer from a horizontal plate facing downward and from a vertical plate.

CHAPTER 2

2.1 EXPERIMENTAL APPARATUS AND INSTRUMENTATION:

The test specimen comprised a rectangular aluminum plate 120 mm long, 60 mm wide and 6 mm thick. The plate was energised by a heater made from 38 SWG nichrome strip wound around a thin mica sheet. For minimising the backward heat losses from the heater, a guard heater was employed and an asbestos sheet of 6 mm thickness was used to separate the two heaters. The guard heater was covered by another aluminum plate 6mm thick followed by a 12 mm thick asbestos sheet. A thin mica sheet was used to insulate each heater from its neighbouring plate. The above units were assembled and held together by epoxy resin, spread around the periphery in a thin layer. Fig. 2.1.1 shows the details of the said assembly.

Eighteen 30 SWG chromel - alumel thermocouples were embeded with an electrically insulating but heat conducting cement (Sauereisen No. DW-30) into 4 mm diameter holes drilled in the test plate. The average depth of these holes was 5.5 mm. Thermocouples B & B' were attached one each to either surface of the asbestos sheet sandwitched between the main heater and the guard heater. Fig. 2.1.2 shows the location of the thermocouples on the test plate. The surface of the test plate was polished with fine emery paper to reduce the heat loss due to radiation.

All dimensions in mm

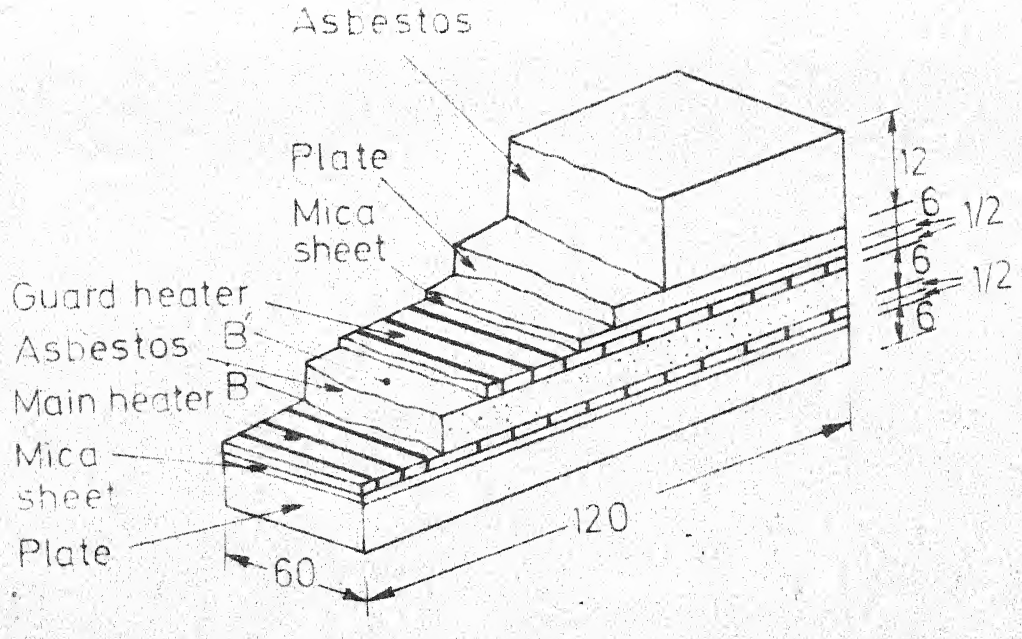

FIG 2.11 TEST PLATE ASSEMBLY

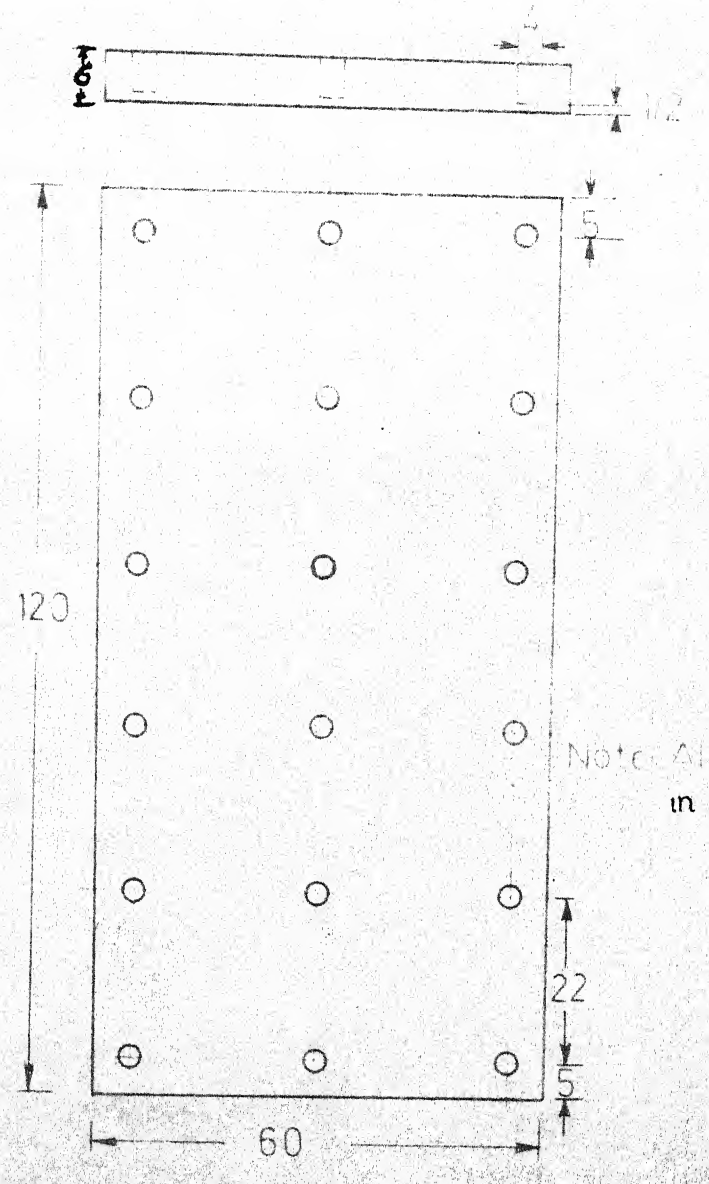

FIG. 2-12 POSITION OF THERMOCOUPLES ON THE TEST PLATE

Stabilized A.C. was supplied to the heaters through a servo-controlled single phase, A.C. voltage stabilizer (Blue-line make) with an accuracy of ± 0.1 percent and was controlled through auto-transformers. The energy input to each heater was measured by noting the current and voltage in each circuit with an ammeter and voltmeter of 0.1 ampere and 1 volt least count respectively. The temperature difference between thermocouples B & B' was controlled and maintained within 0.25°C by regulating the electric input to the guard heater. At steady state the maximum backward heat loss from the main heater was estimated to be negligible (of the order of 0.05 percent of the heat supplied to it). Thermocouple readings were measured with a millivolt potentiometer (Leeds and Northrup, No. 8686). The potentiometer was connected to the various thermocouples through a series of selector switches. The circuit diagram for thermocouple connections is shown in Fig. 2.1.3.

The test plate was kept horizontal with the help of a dial gauge placed on a surface plate levelled with four levelling screws and a 12 inch spirit level. The test plate was kept at various desired inclinations with the help of a vernier protractor of 1 minute accuracy.

2.2 SCHLIEREN METHOD:

2.2.1 Introduction

Numerous methods are available to visualize the flow past models under test. These include the use of tufts, smoke, and oil film placed on

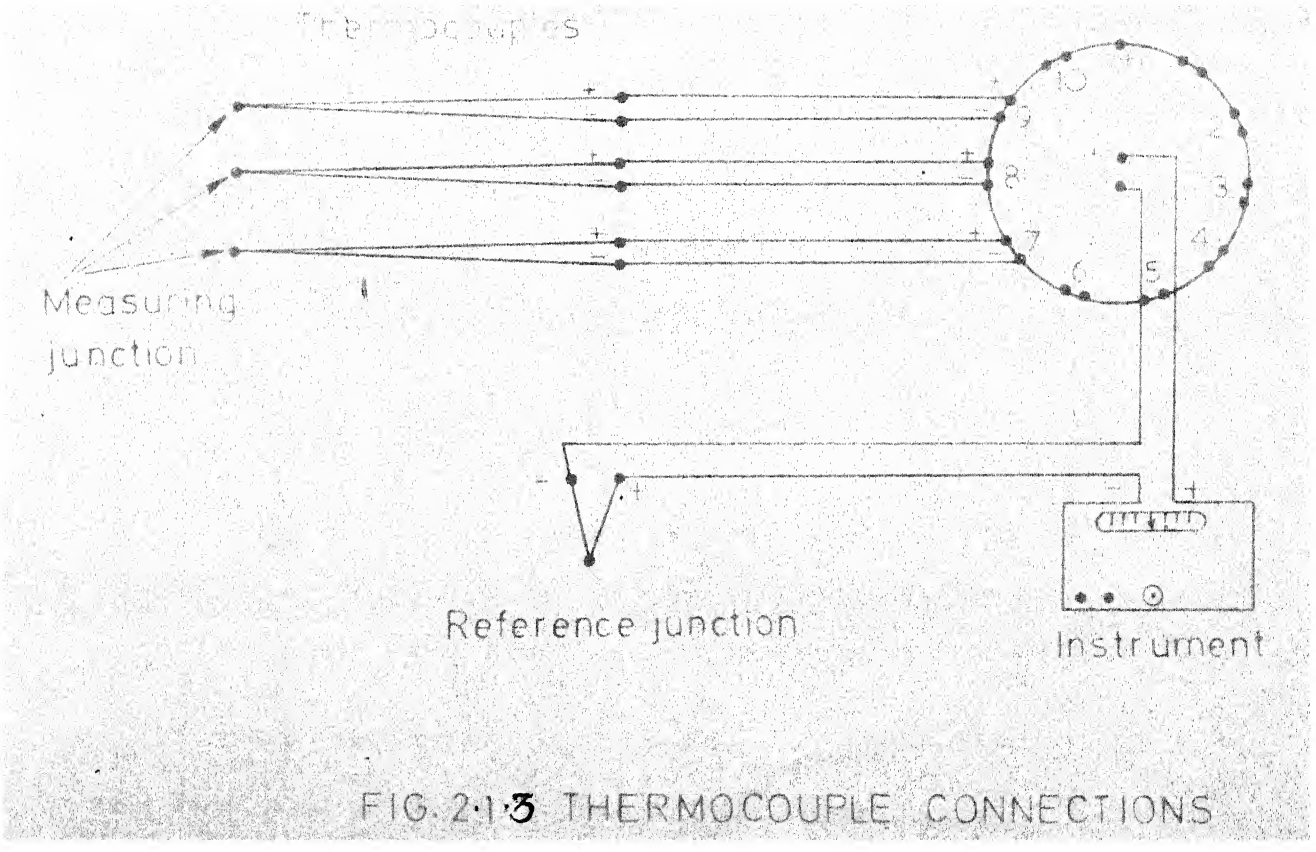

FIG. 2·1·3 THERMOCOUPLE CONNECTIONS

the surface of the model, and the vapour-screen and tuft - grid techniques for observing the vortex pattern behind the model. Among these techniques the schlieren method is most extensively used in high speed and slow speed boundary layer flows, as well as in natural and forced convection heat transfer studies.

This method gives a picture of the flow, caused by changes of refractive index, due to density variations in the flow past the model. The refractive index, n , of the gas is related with sufficient accuracy to its density, ρ , by the equation

$$n - 1 = k'\rho$$

where k' is a constant for a particular gas and for a particular wave-length of light. For air, the equation can be conveniently written as :

$$n - 1 = k'\rho / \rho_o ,$$

where ρ_o is the density at normal temperature and pressure. The factor k' is dimensionless, and for air, varies between 0.000290 and 0.000298 for the visible light spectrum.

If in the working section, there is gradient of refractive index normal to the light rays, the rays will be deflected as the light travels more slowly where the refractive index is larger as given by the equation :

$$C = C_{va} / n ,$$

C_{va} being the velocity of light in vacuum. The deflection of light rays is a measure of the first derivative of density with respect to distance i.e. the density gradient. The variation of refractive index gradient

normal to the rays will differ so that they will converge or diverge, giving increased or decreased illumination on the screen.

In this work the schlieren technique has been used to visualise flow pattern on a heated plate facing downward and inclined at angles of 0, 45 and 90 degrees with the vertical. One can say that this method gives a qualitative picture, showing different regions of varying density in a fluid flow past a model.

2.2.2 Arrangement of the Apparatus :

A typical apparatus used for the present work is shown in Fig. 2.2.1. The light source, S , is placed at the focus of concave mirror, M_1, so that the working section is illuminated by a parallel beam of light. A plane mirror, P_1 , has been introduced into the path of the beam between S and M_1 to fold the light beam. A second concave mirror, M_2, placed beyond the working section, produces an image of the source in its focal plane, K , and there the knife-edge is introduced. Again, a second plane mirror, P_2 , is used to fold the beam emerging from the mirror, M_2.

2.2.3 Apparatus Setting :

The procedure for setting up the schlieren system is simple, but depends to some extent on the nature and arrangement of the apparatus and on the type of flow which is to be observed. For the present work with the described arrangement, the following procedure was adopted.

FIG. 2-2 1 SCHEMATIC DIAGRAM OF SCHLIEREN APPARATUS

The first adjustment that is made is to locate the light source, S, at the focus of the first mirror, M_1. The mirror, P_1, is adjusted such that the beam of light emerging from S and received by it, is directed towards the mirror M_1 to fill its aperture completely. Now the mirror M_1 is adjusted with the help of screws attached at its back to direct a parallel beam of light through the working section. To facilitate the location of S at the focus of mirror M_1, a plane mirror is held between, M_1 and M_2 so as to redirect the beam of light back along its path, from M_1 to P_1, and then to S. An image of S is thus obtained, very close to the original source. If the size of the image is the same as that of the true source, one is sure that S is at the focus of mirror M_1.

The second mirror, M_2, is next moved laterally or vertically until it is filled by the parallel beam emerging from the working section, and is rotated until the light reflected from it, is received by the plane mirror, P_2. Then the mirror P_2 is adjusted to direct the beam of light through the knife-edge assembly.

The knife-edge is now inserted in the focal plane of second mirror and is adjusted until the screen darkens as uniformly as possible when the edge is traversed across the image of the light source. The edge is then so set that a certain fraction of the image of the source is cut-off. Now the apparatus is ready for the visualisation of flow patterns around the model introduced into the working section.

2.3 INTERFEROMETRIC METHOD:

2.3.1 Introduction :

The interferometric method is very useful in the study of gas-flow problems as it provides quantitative as well as qualitative results in the form of a photographic record that can be studied at leisure. The method depends upon the principle of interference of two coherent beams. It is well-known that interference can occur if light beams from two sources emitting waves of equal amplitude and of constant phase difference are combined under suitable conditions. In the present work, the Mach-Zehnder interferometer has been used to produce the interference fringes.

2.3.2 The Mach-Zehnder Arrangement :

The basic arrangement of the Mach-Zehnder interferometer is shown in Fig. 2.3.1 Light from a source, S, is made to impinge with maximum intensity on a source mirror, SM, with the help of collimating lens system, CL. The source mirror, SM, is suspended vertically with the help of a thin wire attached firmly to the main frame. The reflected divergent beam from the source mirror is directed towards the parabolic mirror, N, which can be adjusted with the help of screws mounted on the back and sides of it. This parabolic mirror now sends a parallel beam of light along the axis of the main frame towards the splitter-plate, E, where it is split into two beams. Part of the original beam of light is reflected by the splitter-plate and part is transmitted by it. This splitter-plate, E, is housed in a retaining ring which is placed between the pivot screws attached to the outer-ring.

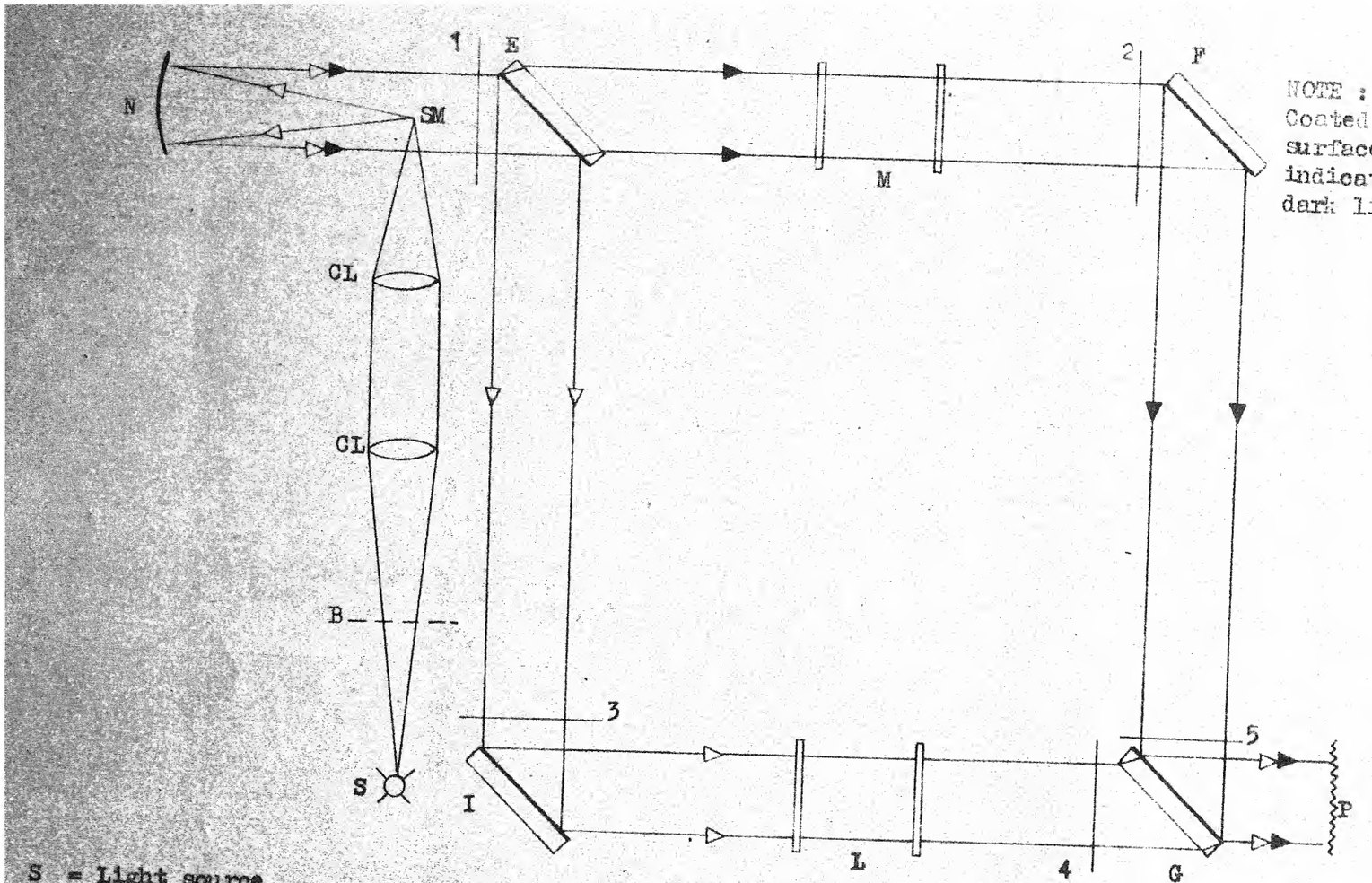

FIG. 2.3.1. Schematic diagram of Mach-Zehnder Interferometer

The outer ring is mounted on the main frame. This plate, E, is kept fixed in its position making an angle of 45° with the axis NE. The transmitted beam from the splitter-plate, E, goes to the mirror F where it is reflected on a second splitter-plate, G, from which it is reflected on the screen or on a photographic plate, P. The mirror F and the splitter-plate G are also mounted in a manner discussed for the splitter-plate E but these can be rotated about either of two axes, horizontal or vertical - with the help of fine - adjustment screws. The light that was reflected by E likewise goes to a fixed mirror, I, from which it is reflected on the splitter plate, G. This mirror has the same mounting arrangement as E, but in addition it can be translated parallel to the axis IG. At G the transmitted part of the beam falls on the screen or on the photographic plate, P.

This arrangement fulfills one of the necessary conditions for the interference of the waves in two beams of light, namely, that the two beams originate from the same light source. From a practical standpoint the arrangement also permits the conditions to be met that the two beams be so widely separated in space that the disturbance to be studied can be introduced into one of the beams without disturbing the other. The disturbance or the 'test section' can, ofcourse, be located anywhere in either of two beams.

2.3.3 Adjustment of the Interferometer :

When the interferometer is first set-up, a number of adjustments must be made in order to obtain fringes and to orient them properly. For the purpose of describing the different adjustments, Fig. 2.3.1 will be referred. It is to be understood that the purpose of alignment procedure is to obtain interference between two coherent light beams which traverse two different paths. In order to accomplish it, the first necessary step is to obtain a collimated light beam, which is described in the following section.

A. Obtaining a Collimated Light Beam :

Before starting this procedure one should be convinced that the light source, filters, condensing lenses, light source mirror and parabolic collimating mirror are at proper positions within the frame which has been installed in thermally stable and vibration free conditions. The light source mirror, SM, should be located on the axis of the main frame, i.e., a line running through the centre of the fixed splitter-plate, E, and the parabolic mirror N. The following steps should be taken serially to obtain the collimated beam.

(1) Turn on the mercury vapour lamp, after adjusting the variac connected in the circuit, so that a voltage of 115 - 120 V is applied to the lamp.

(2) The position of the condensing lenses, CL, is now to be adjusted by moving them on the scaled bench. The important thing to be observed is that the light beam should impinge on the light source mirror, SM, with maximum intensity. This is facilitated by holding a small strip of paper just behind the source mirror, SM, to see when the most intense light spot appears on the mirror.

With the proper orientation of the source mirror the light from the lamp should now fall on the parabolic mirror, N, and a disc of light should be visible in the enclosed frame of the instrument. The intensity and location of the disc of light can be examined by placing a piece of paper in the centre of the frame at the partition (2), Fig. 2.3.1.

(3) To get the disc of light in the centre of circular opening at position (2), an adjustment of the screws mounted on the back and sides of the parabolic mirror is needed.

(4) Readjustment of the orientation of the source mirror, SM, and possibly of the positions of the optical bench assembly, may be necessary so as to get uniform illumination on the paper at position (2).

(5) To facilitate further adjustments, a 5 cm diameter hole made in a piece of paper should be taped at the partition (1) and the hole should be centered as closely as possible with respect to

the partition cut out. There should now be a 5 cm diameter disc of light at the centre of the paper at the position (2). This disc will not be centered with respect to the circular cut out of the frame when either the parabolic mirror N is not located at the axis of the frame or the source mirror, SM, is not on the optical axis of the parabolic mirror. In that case, steps (3) and / or (4) must be repeated. If the disc is not 5 cm in diameter, the light source mirror, SM will not be at the focal point of the parabolic mirror. This necessitates step (6).

(6) Using the adjusting screws on the back of the parabolic mirror, N, move the mirror forward or backward until the illuminated spot is 5 cm in diameter. At this point the light beam coming from the parabolic mirror should be parallel and coincident with the axis of the instrument.

B - Adjustment of the Plane Mirrors :

In the mirror mount assemblies, the plane mirrors F and G, can be rotated about two axes which shall be referred to as horizontal and vertical axes. Extreme care is needed in handling these mirrors so that no scratches or finger prints appear on them.

The planes of the outer ring of the splitter plates and the mirrors should be adjusted to make an angle of 45° with the base of the mount. It is understood that E, F, G and I, have been already mounted into proper positions with fixed measured distances between them.

During the following adjustments the piece of paper with 5 cm diameter hole should still be in position (1).

(7) Place a screen at the position (3). It will be possible to note the size and location of the light beam coming from splitter-plate, E. Note that if the diameter of the light disc is not the same as that of the hole in the paper at position (1), the instructions in Step 6 have to be repeated.

(8) The inner ring of the splitter-plate mount E should be rotated about its axis until the vertical location of the light disc is centrally located with respect to the cut-out in the frame at (3).

(9) Now, the translating mirror is to be adjusted at position I. The light beam from E should be centered on the mirror surface after removing the screen from the position (3).

(10) If the light beam is not centered, the splitter-plate, E, may be moved by loosening the screws in the base of the yoke and sliding the entire yoke assembly until the beam is centered on the mirror at I.

The screen should now be placed at the port at point (4).

(11) By swinging the mirror, I, about its horizontal axis the light should be centered vertically with respect to the cut out at (4).

(12) The distance of mirror, F, with respect to the splitter-plate, E, should be made exactly double the distance between E and I. The distance should be measured between the centers of pivot screws, provided on the top of E, F, G and I. Now remove the screen at (4).

(13) The light should be centered vertically by swinging the mirror, F, about its horizontal axis.

(14) Now, the splitter-plate, G, in the interferometer frame should be adjusted to the proper orientation as stated earlier with the ground glass screen at position P. Two source images should be visible, one image coming through the test section and the other through the enclosed reference section.

(15) It may be necessary to adjust the mirrors, first at G, then at I and F to bring the images into coincidence.

C - Fine Adjustment:

This procedure requires a telescope mounted at P such that two images of the source mirror are visible through it. The adjustments are made as below :

(16) The telescope should be set up by looking along the axis of the instrument and adjusted in such a fashion that the front of the small light source mirror comes into focus. In general there will be two images of the source mirror because of the inexact

initial adjustment process. The aim of the fine adjustment process is to obtain two beams of light which appear to originate from a single source. (This portion of the adjustment may be carried out by decreasing the intensity of light by placing the filters before the lamp as too high an intensity is harmful to the eyes).

(17) The two images can now be made to coincide with the adjustments of mirror, F, or splitter-plate, G. With the coincidence of these two images, it might be possible to see the fringes but usually the two beams will get diverge at too large an angle, thus making the fringes invisible.

(18) In order to reduce the angular divergence of the beams, the telescope may be focussed progressively on points farther than the source. For this purpose it is often necessary to introduce another object in the light path between E and N, i.e., at or near the back of source mirror, say the screen with 5 cm cut-out at (1). The back of the light source mirror and the screen at (1) will probably at first appear as a double image. The object is now to obtain progressively a single image of the front and back of the source mirror in each of the two focussing planes. This is accomplished by rotating either mirror F or G, <u>always using the same mirror adjustment to cause the coincidence of</u>

the same image. That is to say, if F is adjusted to make the two images of the front of the source mirror coincident, the same mirror should be adjusted always for the image appearing in the plane of the front of the source mirror.

The steps involved are :

(a) focus on the front of the source mirror,

(b) adjust splitter-plate, G, to make image coincident,

(c) focus now on the cut-out at (1), i.e., at the back of source mirror,

(d) adjust the mirror, F, to make the images coincide at this plane.

If the above steps are repeated several times, one of two things will become apparent. Either the adjustment will appear to be converging, (i.e., the images will come closer together) or the adjustment will become worse. If the latter is the case then the mirror F should be adjusted for the front image of the source mirror and G for the cut-out, and the same procedure repeated. Unfortunately, it is not possible to guess in advance which mirror is to be adjusted first, to get the images to coincide. For the final fine adjustment, the fine knobs on the frame for mirror F and G may be used.

Now as the fine adjustment process converges, dark lines start to appear on the front face of the source mirror and they will appear to

get darken and farther apart as the fine adjustment approaches the end. The fine adjustment procedure may be continued until a single dark line is visible on the front of source mirror. At this stage the fine adjustment controls should be operated very carefully with maximum precision. After obtaining a single fringe at the front of the source mirror, the telescope should be focussed at the back of source mirror to attain the maximum density fringes in the field at this position.

(19) For the control of darkness of fringes the splitter-plate, G, and for the spacing and orientation of fringes the mirror, F, should always be adjusted.

Now after obtaining the fringes in the field, it is necessary to obtain the zero-order fringe pattern which can be obtained by following the procedure given below.

D - Zero-Order Fringe Adjustment :

(20) Remove the filter elements from the bench and see whether the fringes are visible or not as this will depend upon how nearly equal the two light paths are in optical effective path length. If the paths are quite different, no fringes will be visible and it will be necessary to translate the mirror mount I to equalize the optical path lengths but there will be no way to know in advance which way the mount should move. The method to determine it is as follows :

(a) Translate the mirror, I, in a particular direction.

(b) Replace the filters.

(c) Observe the movement and intensity of green light fringes. If they appear to be becoming less distinct, and if removing the filters, does not yield fringes, the direction of translation of mirror has been wrong.

(d) Reverse the direction of translation of the mirror and see whether the fringes are visible in both filtered and unfiltered mercury light.

(21) With the introduction of white light only a few black fringes will be observed. Mirror I is to be adjusted to make these fringes appear with the greatest contrast. At this stage, if green light is introduced, the fringes with even greater contrast and more visibility will be obtained.

With the unfiltered mercury light, every 6th or 8th fringe is darker than the rest. When one of these dark fringes coincides with the zero-order fringe, it is as black as a green light fringe. Thus the mount I is moved and the darkness of the fringes is observed. If the contrast of the fringes increases, the translation is in right direction. When the contrast of the fringes indicates that the zero-order fringe is approaching, the check with whitelight should be made each time a new fringe appears in the field. This will prevent passing over the zero-order fringe.

Now the instrument is ready with final adjustment for viewing interferometric patterns in free convection flows

E - Zero - Order Fringe Adjustment with a Laser Beam :

The final setting of the interferometer for the present work has been carried out with a laser beam (Spectra Physics Helium - Neon stabilite No. 120) as it is monochromatic and spatially coherent. The beam is intense enough to get a bright and sharp interference - fringe - pattern which can be photographed very easily. The use of the laser beam requires a beam - expander which can expand the beam to the required degree.

The beam expander consists of a microscope objective and a pin - hole filter of the size of a few microns, mounted together in a frame such that the microscope objective may be moved relative to the filter. A mechanical arrangement for the adjustment of the pin - hole exactly in front of the objective so as to pass the beam is necessary. The microscope objective of the required magnification (45 X for the present work) expands the laser beam.

Adjustment Procedure :

The adjustment procedure to get the zero - order fringe pattern is as follows :

(1) Remove the mercury light source and install the laser along the axis of the condensing lens assembly.

(2) Switch on the laser, and try to get the beam to converge on the source mirror, SM, with the condensing lenses in position. This can be done by lowering or raising the level of laser and displacing the laser in a horizontal plane. This adjustment can be facilitated by the use of a screw-jack.

(3) After the completion of step (2) it is necessary to observe that the beam reflected back from the parabolic mirror, N, should fall at the centre of splitter plate, E. This can be observed by holding the piece of paper at position (2) Fig. 2.3.1. If the beam does not fall at the centre of the paper, it indicates that the beam does not make a proper angle of incidence at the source mirror and consequently step (2) is to be repeated.

(4) Introduce the beam expander between the laser and the condensing assembly, maintaining the microscope objective towards the laser and adjust the pin - hole so that the expanded beam fills the aperture of condensing lens system.

(5) Adjust the condensing lenses, without distrubing the laser, on the scaled bench to get the converged beam at the source mirror.

(6) As soon as the step (5) is complete, fringes will be visible at P, provided the mirrors and splitter plates are previously adjusted as in steps 7 - 15 (see Sec. 2.3.3, B).

(7) Now the aim of the adjustment is to get sharp fringes with a maximum of spacing and proper orientation. For spacing, mirror G is adjusted while mirror F is adjusted for orientation.

(8) Translate the mirror, I, in one direction say backward, and observe the contrast and spacing of the fringes. If contrast and spacing increase, the translation is in the right direction, otherwise, reverse the direction of translation and obtain a sharp fringe - pattern with maximum fringe spacing.

(9) The set-up is ready for obtaining an interferogram.

2.4 EXPERIMENTAL PROCEDURE :

The test plate assembly is held at the desired inclination in the test section of Mach-Zehnder interferometer as shown in Fig. 2.4.1. The most important adjustment consists in bringing the axis of the beam of the light to grazing incidence at the hot surface of the test section. After the completion of this step, the assembly is fixed rigidly in this position throughout the test.

The plate is then heated by switching on the main heater and the guard heater. It is not known in advance what combination of electric input to the two heaters will make the difference of the thermocouple readings B & B' very nearly disappear. So this is done manually by trial and error. It took approximately 8-10 hours to achieve the

above mentioned condition of negligible temp. drop. As soon as the steady state is obtained, the readings of the various thermocouples are noted with the help of millivolt potentiometer and a photograph of the fringe pattern is taken.

The next set of readings is taken with the model at the same inclination but at higher temperature of the surface of the plate. Tests similar to the above were carried out with the plate inclined at angles of 0, 30, 45, 60 and 90 degrees to the vertical respectively and the corresponding fringe patterns are shown in Fig. 2.4.2.

Next the test plate is examined on the Schlieren apparatus for flow visualization. A photographic sheet film is held in a plate mounted on a camera to capture the graphic view of the undisturbed flow-pattern by applying the proper cut-off by the knife edge. Slow speed with high contrast film was used. Schlieren photographs were taken with the plate surface at 0, 45 and 90 degrees with the vertical as shown in Fig. 2.4.3.

2.5 EVALUATION OF INTERFEROGRAMS :

Figure 2.5.1 is the schematic sketch of a fringe pattern. If the temperature were uniform throughout, the center line of the fringe A instead of that of B would pass through the point P. The shift of one fringe at this point P indicates that there is one less wave of light in the path through P than there would be if the temperature at P were the same as at Q.

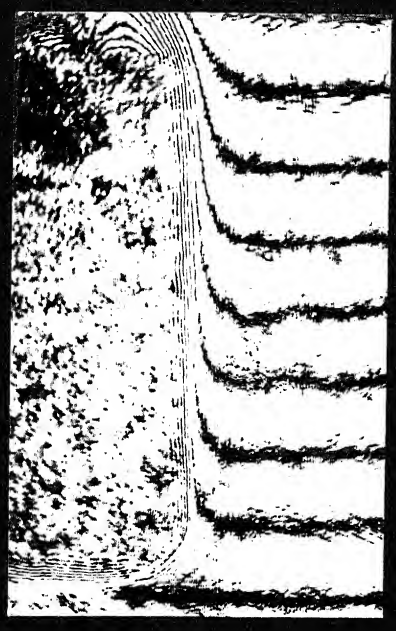

(a) $\theta = 0°$, $t_w = 93.6\ C°$

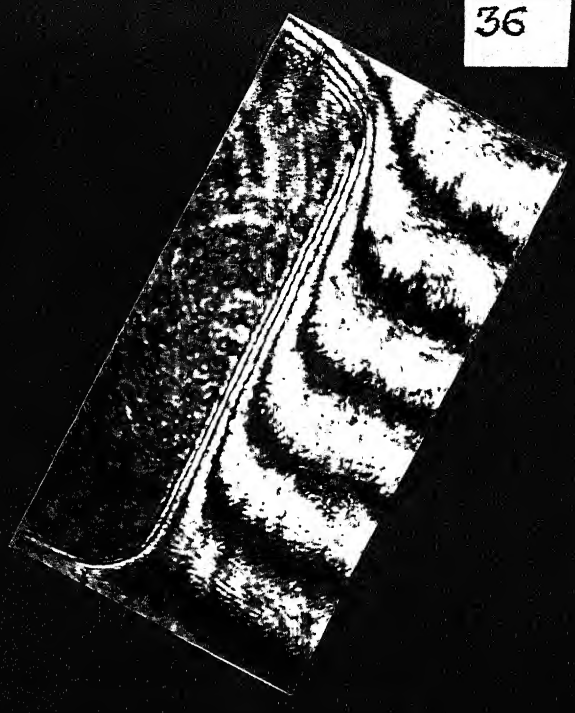

(b) $\theta = 30°$, $t_w = 59.5\ C°$

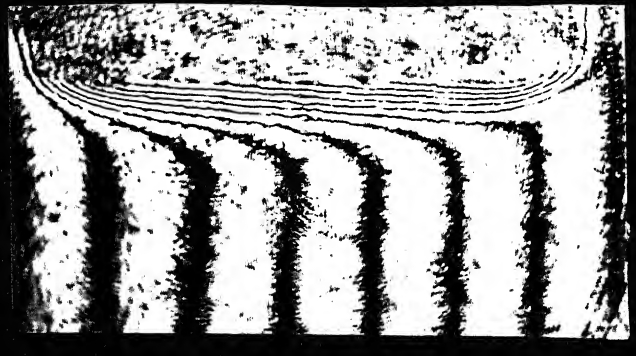

(c) $\theta = 90°$, $t_w = 71.6\ C°$

FIG. 2.4.2. FRINGE PATTERNS AT VARIOUS PLATE ANGLES AND SURFACE TEMPERATURES

(d) $\theta = 30°$, $t_w = 63.3\ C°$

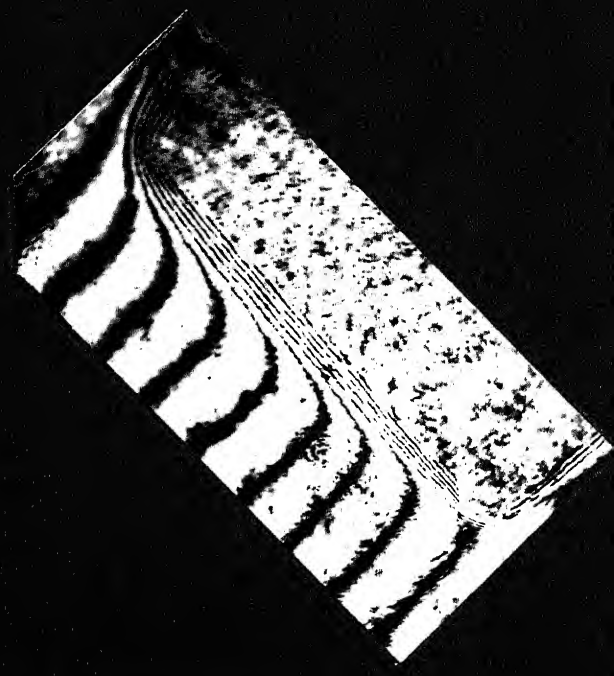

(e) $\theta = 45°$, $t_w = 77.5\ C°$

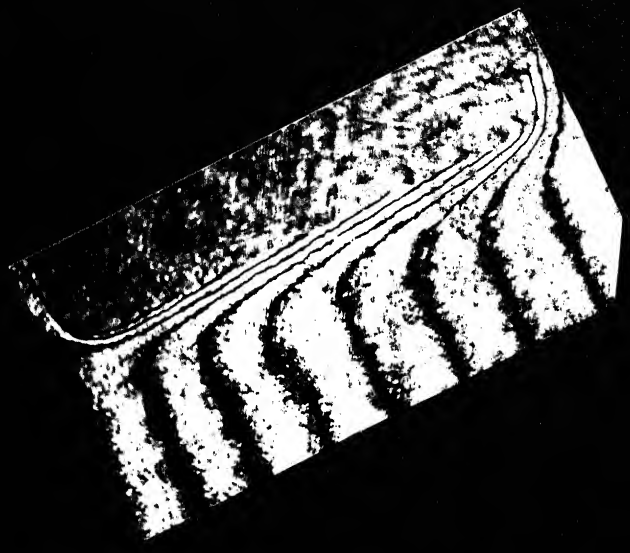

(f) $\theta = 60°$, $t_w = 62.0\ C°$

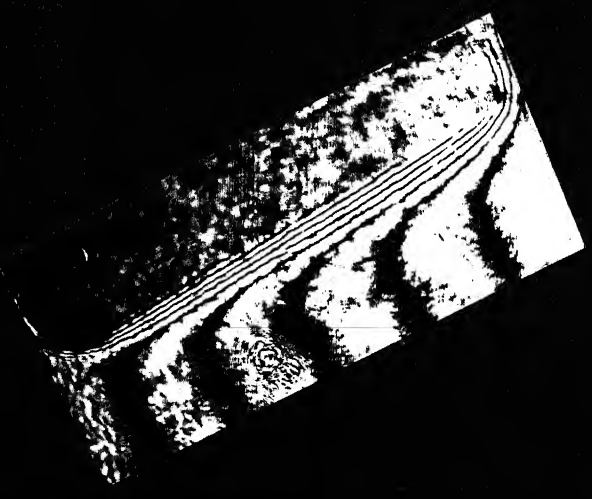

(g) $\theta = 60°$, $t_w = 67.7\ C°$

FIG. 2.4.2. FRINGE PATTERNS AT VARIOUS PLATE ANGLES AND SURFACE TEMPERATURES

(a) $\theta = 90°$, $t_w = 110.5\ C°$

(b) $\theta = 0°$, $t_w = 94.7\ C°$

FIG. 2.4.3. SCHLIEREN PHOTOGRAPHS SHOWING THERMAL BOUNDARY LAYER

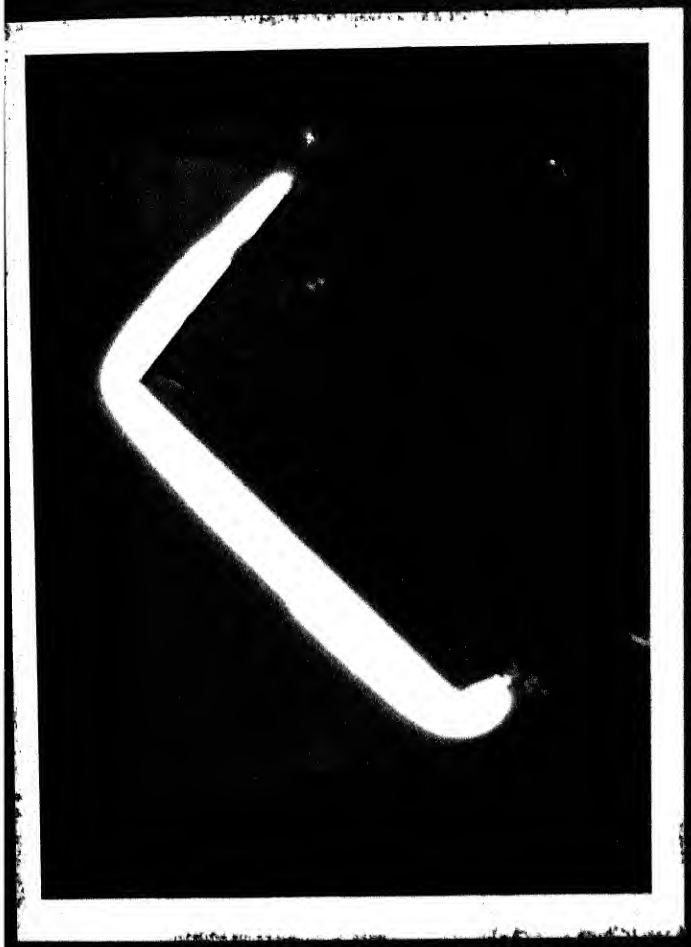

(c) $\theta = 45°$, $t_w = 75.3\ C°$

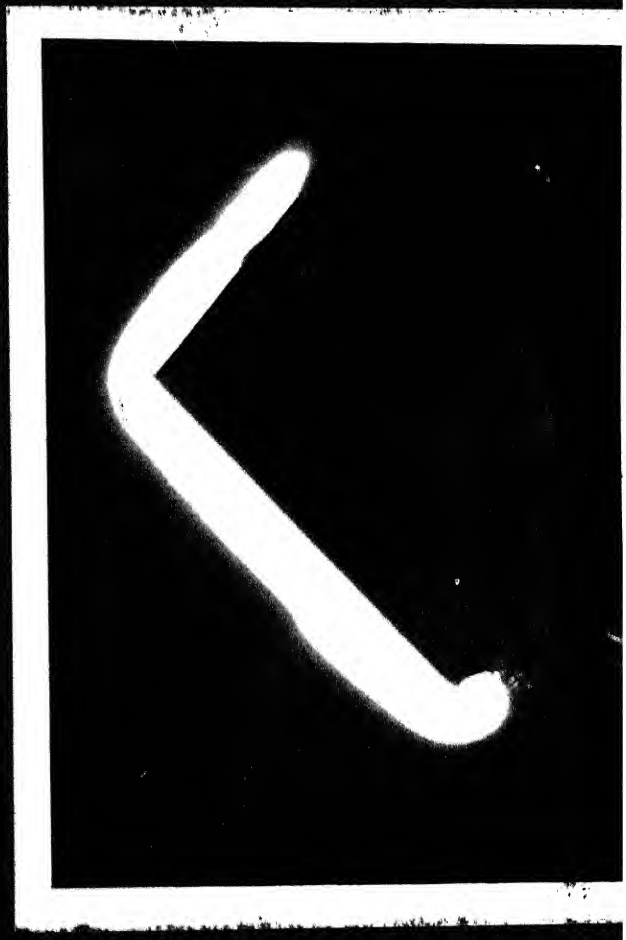

(d) $\theta = 45°$, $t_w = 94.2\ C°$

FIG. 2.4.3. SCHLIEREN PHOTOGRAPHS SHOWING THERMAL BOUNDARY LAYER

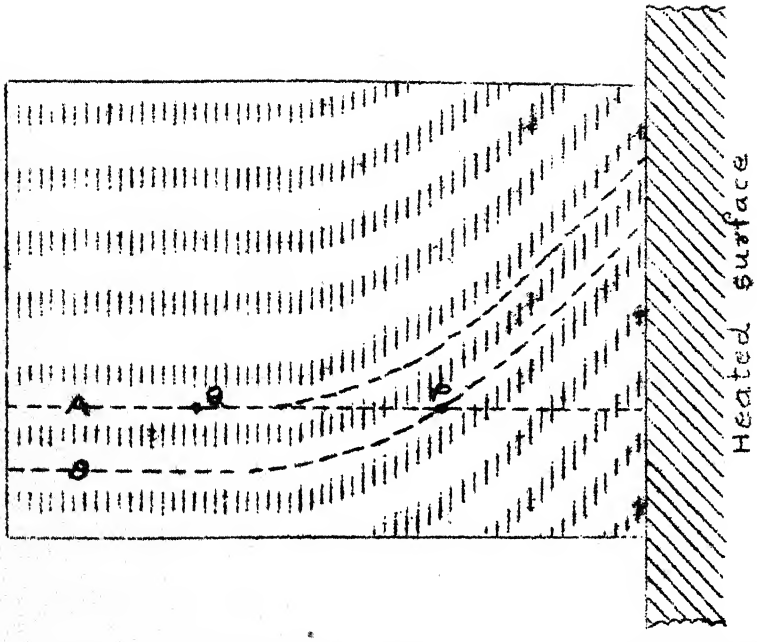

Fig. 2.5.1 SCHEMATIC SKETCH OF A FRINGE PATTERN

The temperature of air is derived from its density which is related with the refractive index by the Lorenz - Lorentz [20] equation

$$\frac{n^2 - 1}{n^2 + 2} = k'' \rho \qquad (1)$$

where n is the index of refraction, ρ the density, and k'' is a constant characteristic of the fluid (air).

Since the index of refraction of air under room conditions is the order of 1.0003, the equation above reduces very closely to

$$n - 1 = 3/2\, k'' \rho \qquad (2)$$

If n_a is the index of refraction of the room air and n_2

the index of refraction of the heated air in front of the plate, and ρ_a and ρ_2 are the corresponding densities, then

$$n_a - n_2 = 3/2\ k''(\rho_a - \rho_2)$$
$$= 3/2\ k''\rho_a\ (1 - \rho_2 / \rho_a)$$
$$= (n_a - 1)\ (1 - \rho_2 / \rho_a) \qquad (3)$$

If l is the length of the path of light under consideration, and if λ_o is the wave length in vacuum of the light used, then the number of wave-lengths, N_o, along this path in vacuum would be

$$N_o = \frac{l}{\lambda_o} \qquad (4)$$

If N_a and N_2 are the number of wave-lengths under consideration, then the index of refraction is given by

$$n_a = \frac{N_a}{N_o} \qquad (5)$$

and

$$n_2 = \frac{N_2}{N_o}$$

Inserting the values of (4) and (5) in equation (3) and re-arranging yields

$$N_a - N_2 = (n_a - 1)\ \frac{l}{\lambda_o}\ (1 - \frac{\rho_2}{\rho_a}) \qquad (6)$$

But for a given pressure,

$$\frac{\rho_2}{\rho_a} = \frac{T_a}{T_2} \qquad (7)$$

Using (7) and representing $(N_a - N_2)$ by ΔN, (6) yields

$$\Delta N = (n_a - 1) \frac{1}{\lambda_o} \left(\frac{T_2 - T_a}{T_2}\right) \tag{8}$$

On solving explicitly for temperature rise above that of room air this equation becomes

$$T_2 - T_a = T_a \frac{\Delta N}{(n_a - 1) \frac{1}{\lambda_o} - \Delta N} \tag{9}$$

Since in the interfero-meter, the change in number of light waves for a given path is equal to the fringe displacement, ΔN, as measured in fringe widths, equation (9) can be used to measure the temperature rise above room air at any point along the center line of an interference fringe. T_a is the temperature of the room air in degrees kelvin and the quantity $(n_a - 1)$ is given in the "International Critical" tables [19] for standard conditions and may be calculated for any other condition by using gas laws. In the present study, fringe shift was measured with an optical projector (Bausch & Lomb make).

CHAPTER 3

3.1 RESULTS AND DISCUSSION OF RESULTS :

3.1.1 Temperature Distribution of the Plate Surface :

Fig. 3.1.1 shows temperature distributions of the plate for the horizontal, inclined ($\theta = 45°$) and vertical orientations. As expected the temperature around the middle of the plate is slightly higher than that towards the edges. The variation in the surface temperature was, however, within $\pm$ 2% of the average temperature of the surface. The surface of the plate was, therefore, assumed to be an isothermal surface.

3.1.2 Schlieren Study :

Fig. 2.4.3 shows the schlieren photographs for horizontal, vertical and inclined ($\theta = 45°$) positions of the heated plate. For the horizontal plate facing downwards, it is clear that the thermal boundary layer is maximum at the center and decreases towards the free edges. The boundary layer at the free edges is not zero as postulated by various authors in their theoretical analyses (Refs. [9], [10], [11], [12] and [13]). The vertical plume from the two sides was also observed by Aihara, et. al. [15]

For the plate inclined at 45° with the vertical, the boundary layer is thicker at the leading edge and thinner at the top. As

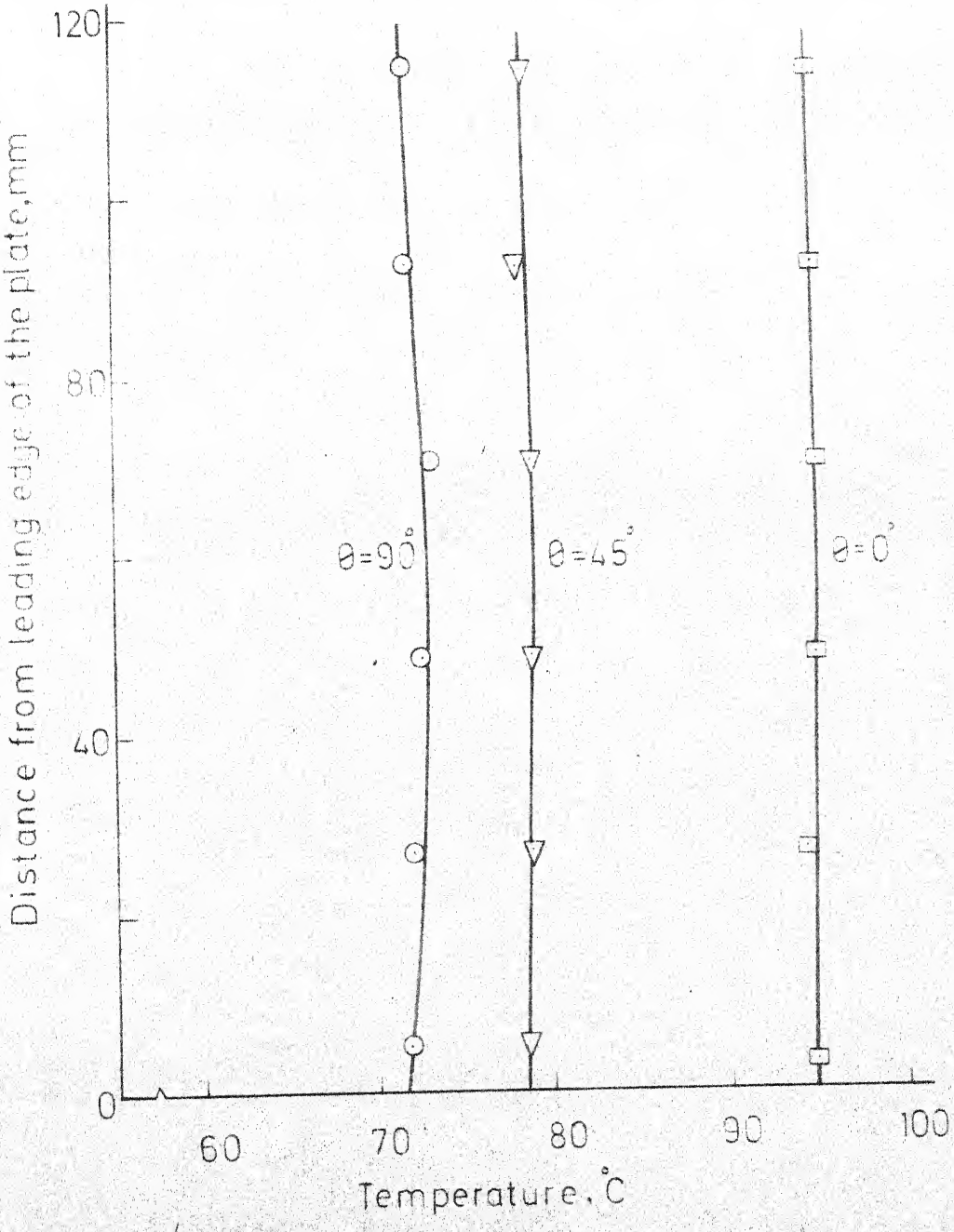

FIG. 3·1·1 TEMPERATURE DISTRIBUTION OVER THE PLATE SURFACE

expected the boundary layer thickness increases with the rise in temperature of the plate.

For the vertical plate, the boundary layer is thinner at the leading edge and thicker at the top. Near the top, the boundary layer bends inwards due to the strong convection currents from the top horizontal edge of the plate. These convection currents increase the heat transfer coefficient from the plate surface.

3.1.3 Interferometric Results :

The photographs of the various fringe patterns obtained are shown in Fig. 2.4.2. These fringe patterns were taken by allowing the image of the pattern to fall on a FORTEPAN 160 ASA sheet film. It is suspected that scratches and dust particles on the mirrors may have resulted in local distortion of the fringes. Temperature distributions for various fringe patterns as calculated from their respective fringe shifts are given in Figs. 3.1.2 through to 3.1.4. The dotted lines have been drawn tangent to the temperature distribution curves at S = 0 and therefore, give the temperature gradients at the plate surface.

3.1.4 Relation Between Local Nusselt Number and Local Rayleigh Number :

(a) Horizontal Plate :

Fig. 3.1.2 shows the temperature distribution below the surface of the horizontally heated plate. The experimental data have been

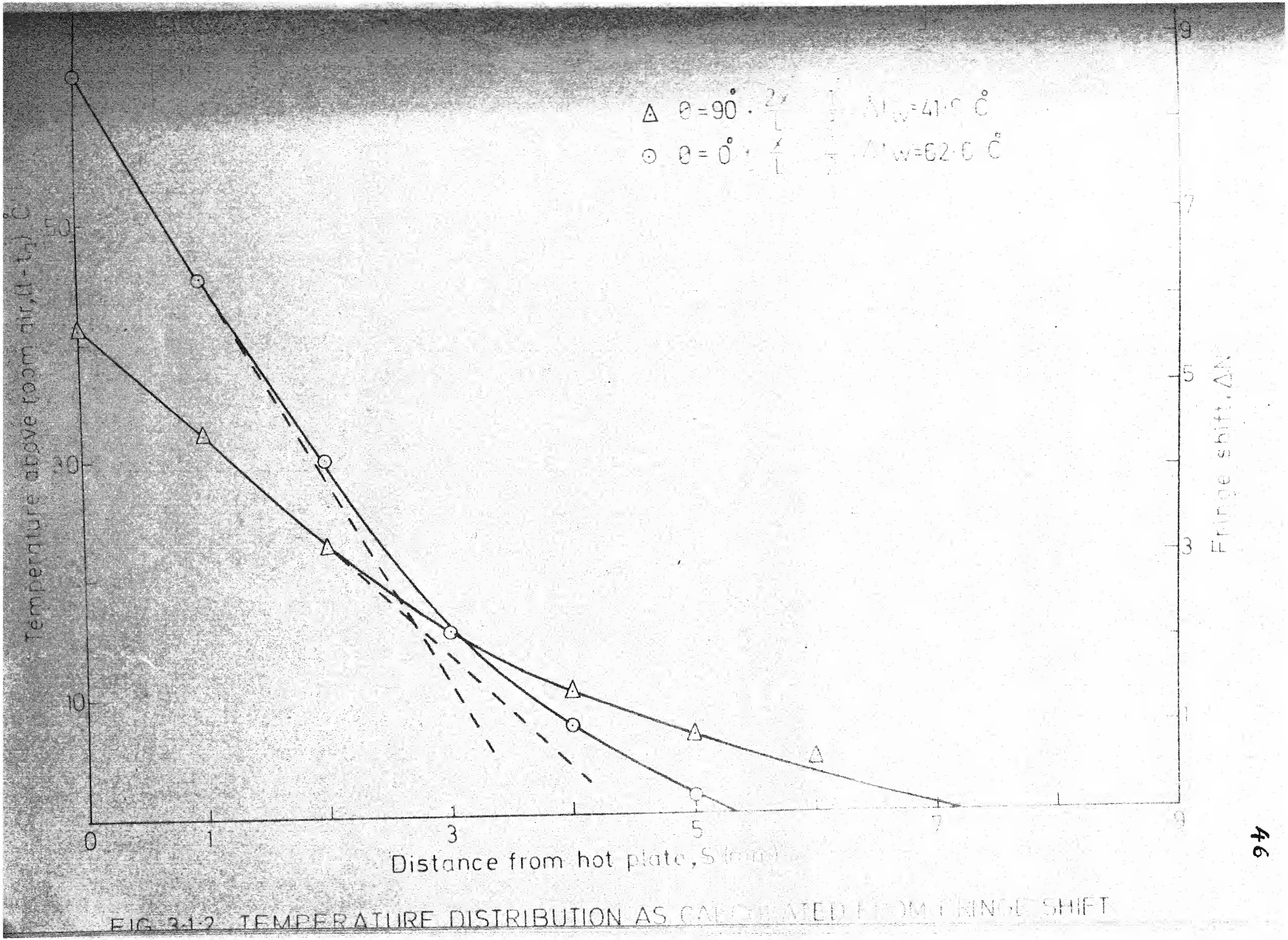

FIG. 3.1.2 TEMPERATURE DISTRIBUTION AS CALCULATED FROM FRINGE SHIFT

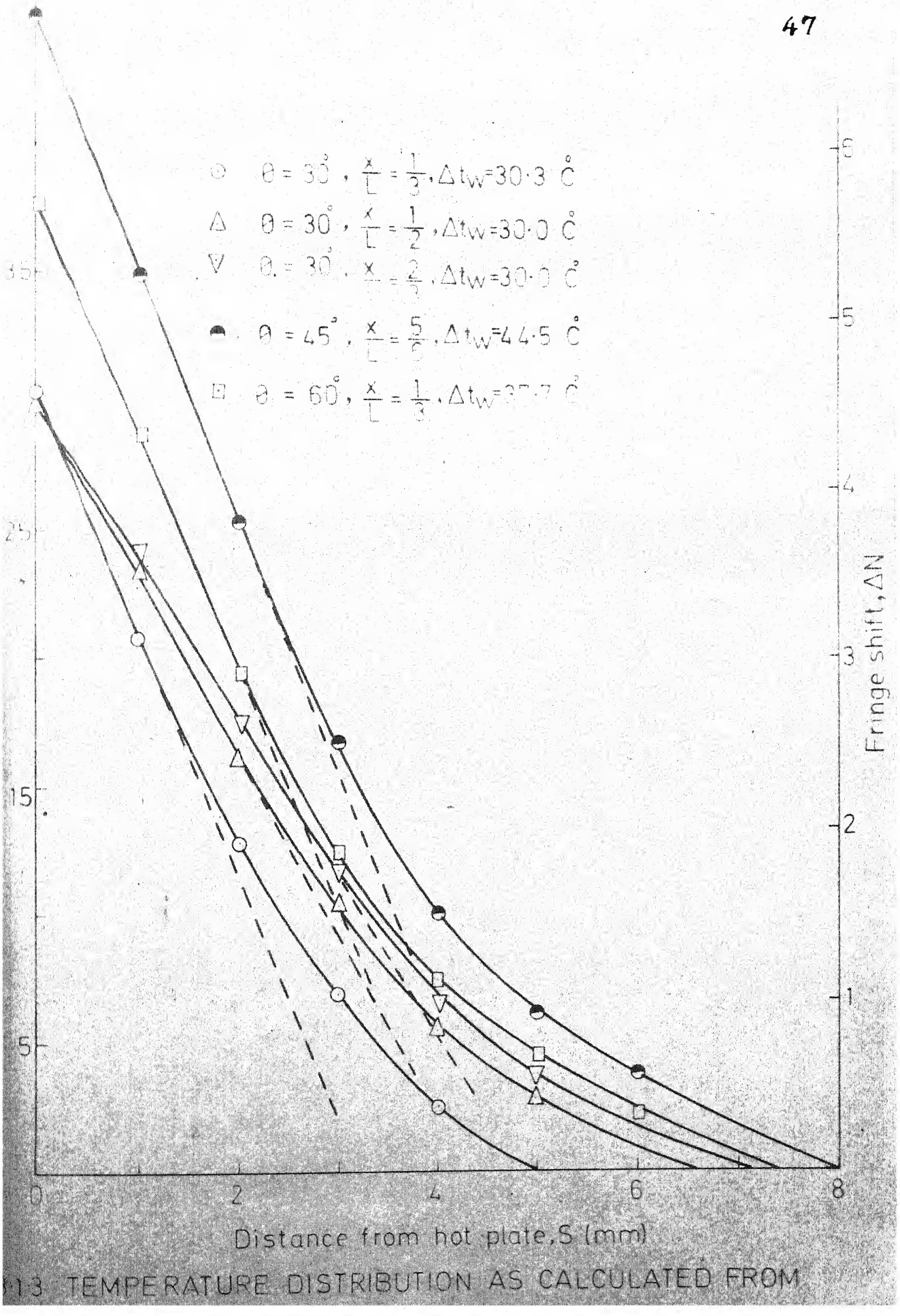

·13 TEMPERATURE DISTRIBUTION AS CALCULATED FROM

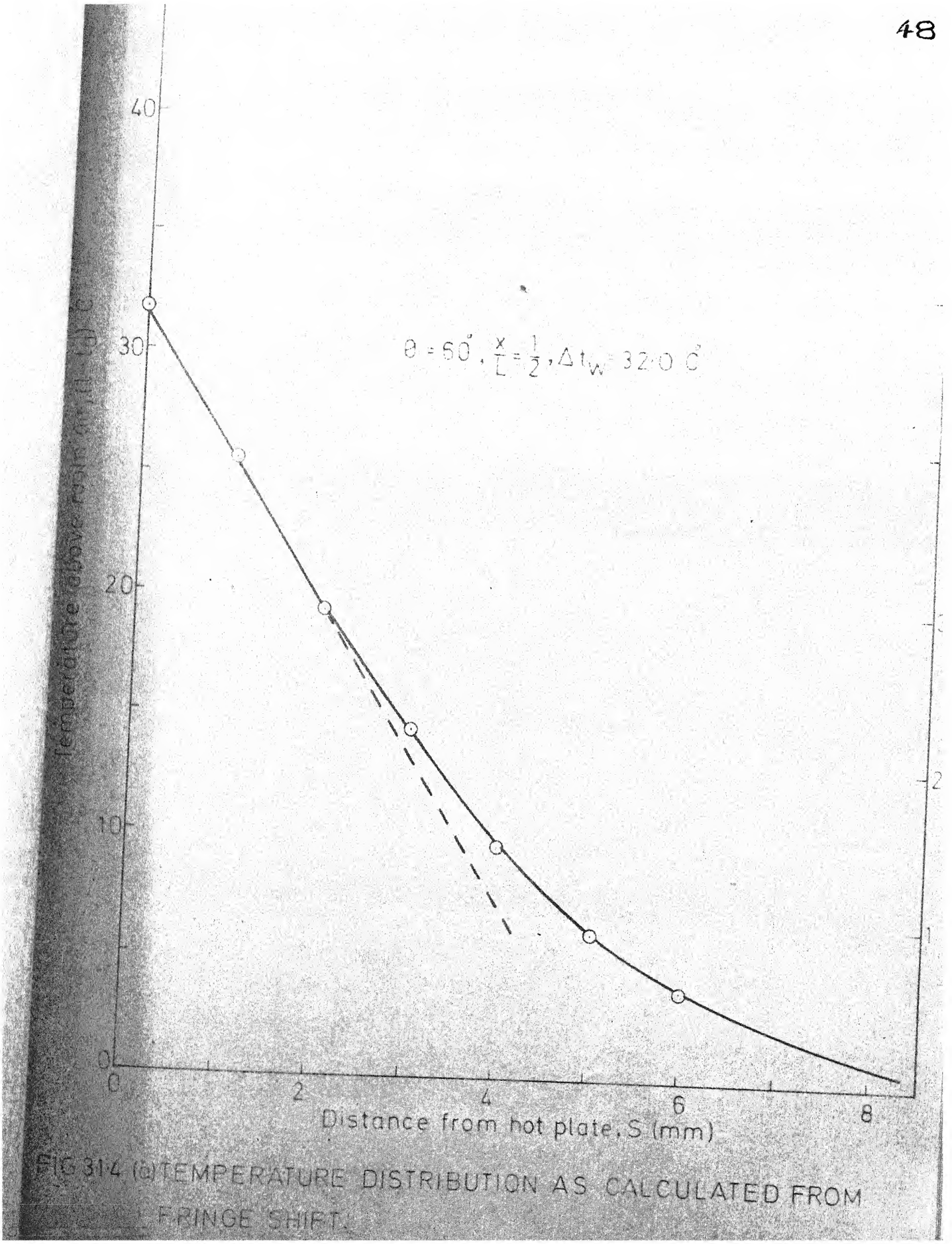

FIG 3·4 (a) TEMPERATURE DISTRIBUTION AS CALCULATED FROM FRINGE SHIFT.

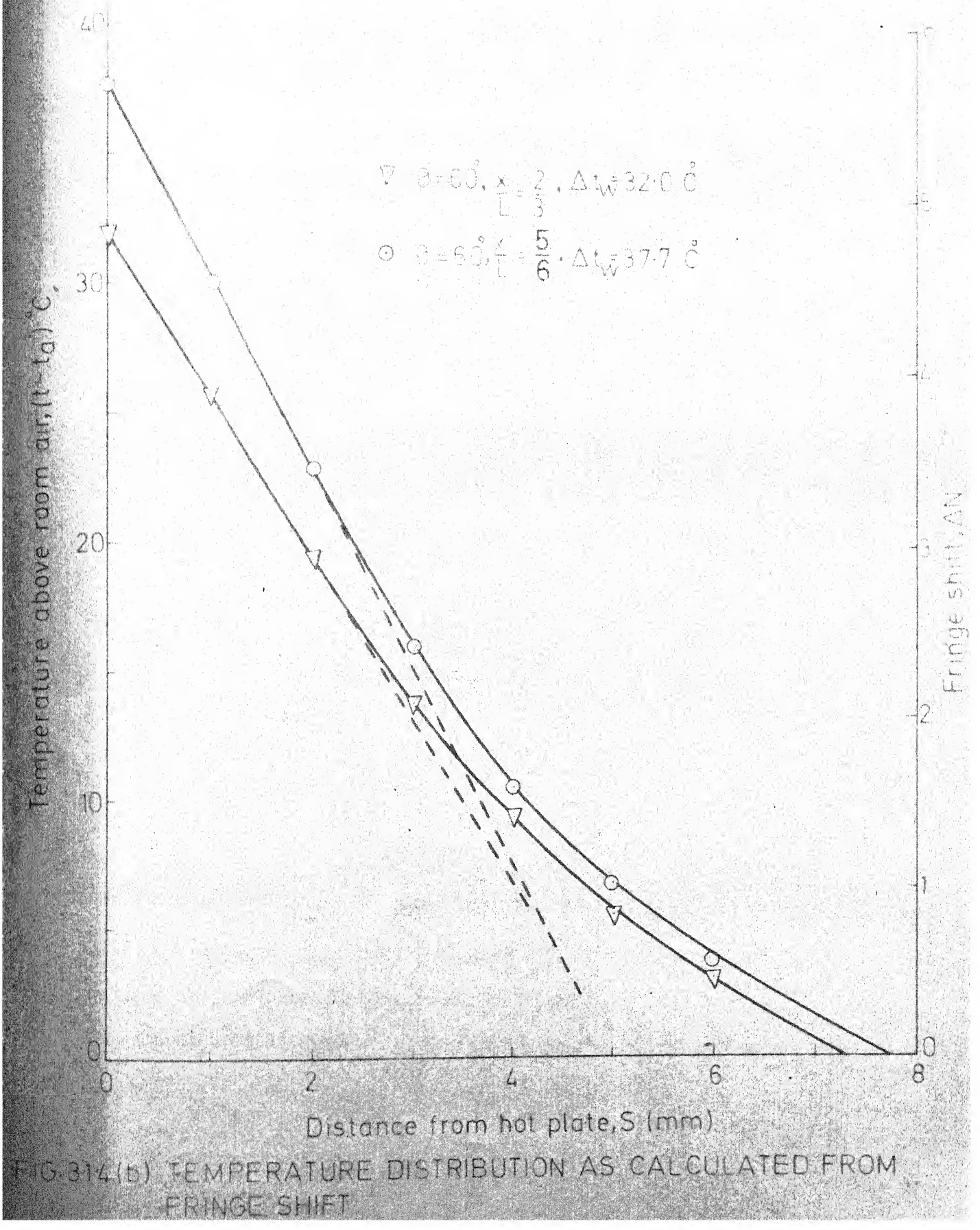

FIG. 314 (b) TEMPERATURE DISTRIBUTION AS CALCULATED FROM FRINGE SHIFT

substituted in the relationship $Nu_x = c_x (R_a)_x^{1/5}$. The 1/5th power of Rayleigh number has been taken from the theoretical and experimental studies made by various researchers in the field (Table 3.1). Average heat transfer coefficients have been computed by integrating the local heat transfer coefficients over the entire characteristic length of the test specimens. Table 3.1 compares the results of the present study with those reported in the literature.

TABLE 3.1 : Comparison of Average Heat Transfer Coefficient for Horizontal Plate Facing Downwards.

Investigator	Plate geometry	Correlation Coefficient (c)
Present study	Rectangular	0.753
Singh, et. al [13] (Theoretical)	Square	0.716
Kadambi [12] (Theoretical)	Circular	0.795
Stewartson [10] (Theoretical)	Infinite strip	0.841
Francisco & Glicksman [16] (Experimental)	Square	0.68
Aihara, et. al. [15] (Experimental)	Rectangular	0.71

As expected, the present experimental results yield heat transfer coefficients which are approximately 5% higher than those predicted by Singh, et. al. [13] and about 10% and 6% higher than those reported by Francisco and Glicksman [16] and Aihara et. al [15] respectively. The discrepancy, it is believed, could be explained

by the fact that the previous authors have invariably assumed or attempted to simulate 2-dimensional flow conditions in their studies by restricting the flow of heat from the two sides of their test specimens. In the present study, however, the plate did not have any restriction on any of its sides. Further, the invalid assumption made by the authors (Table 3.1) in their theoretical analyses, that the boundary layer thickness is zero at the free edges, is bound to result in lower heat transfer coefficients. On the contrary, the vertical plume at the edges as observed by Aihara, et. al [15] and confirmed by the present series of tests on the horizontally heated plate facing downwards helps in increasing the heat transfer coefficients.

(b) Inclined Plate Facing Downwards:

Fig. 3.1.3 and 3.1.4 show the temperature distributions for the various inclined positions of the plate facing downwards. It is evident from these graphs that as the surface temperature of the plate increases, the thermal boundary layer also increases. The experimental data were substituted in the correlation $Nu_x = c_x (Gr. Pr. Cos \theta)^m$ as proposed by Rich [17] . The value of the exponent m was, therefore, taken as 1/4, the same as that for a vertical plate. Appendix-B shows a sample evaluation of the local Nusselt number.

Table 3.2 gives the range of the experimental data and the local Nusselt numbers obtained in this study. The data for the vertical

plate have also been included in the present investigation, treating $\theta = 0°$ as the limiting case.

TABLE 3.2 Experimental data and Local Nusselt Numbers obtained for Inclined Plate Facing Downwards.

θ (degrees)	Plate temperature (c°)	x/L	Gr_x	Pr_x	Nu_x	c_x	$c = \frac{4}{3} c_x$
0	93.6	1/2	1.52×10^5	0.6960	8.16	0.454	0.6053
30	59.5	2/3	1.89×10^5	0.6985	8.42	0.458	0.6107
		1/2	1.79×10^5	0.6985	6.75	0.455	0.6066
30	63.3	1/3	2.42×10^4	0.6980	6.24	0.567	0.7560
45	77.5	5/6	6.25×10^5	0.6970	10.80	0.458	0.6107
60	62.0	2/3	2.19×10^5	0.6985	7.81	0.469	0.6250
		1/2	9.20×10^4	0.6985	5.86	0.437	0.5827
60	67.7	1/3	3.03×10^4	0.6980	4.88	0.443	0.5906
		5/6	4.74×10^5	0.6980	9.85	0.487	0.6480

Average $c = 0.626$

From the results of Table 3.2, the proposed correlation for inclined flat plate facing downwards becomes

$$Nu = 0.626 \, (Gr. \, Pr. \, Cos\theta)^{1/4}$$

Fig. 3.1.5 compares the experimental data from the inclined flat plate facing downwards with the theoretical and experimental results obtained from the literature. Heat transfer coefficients

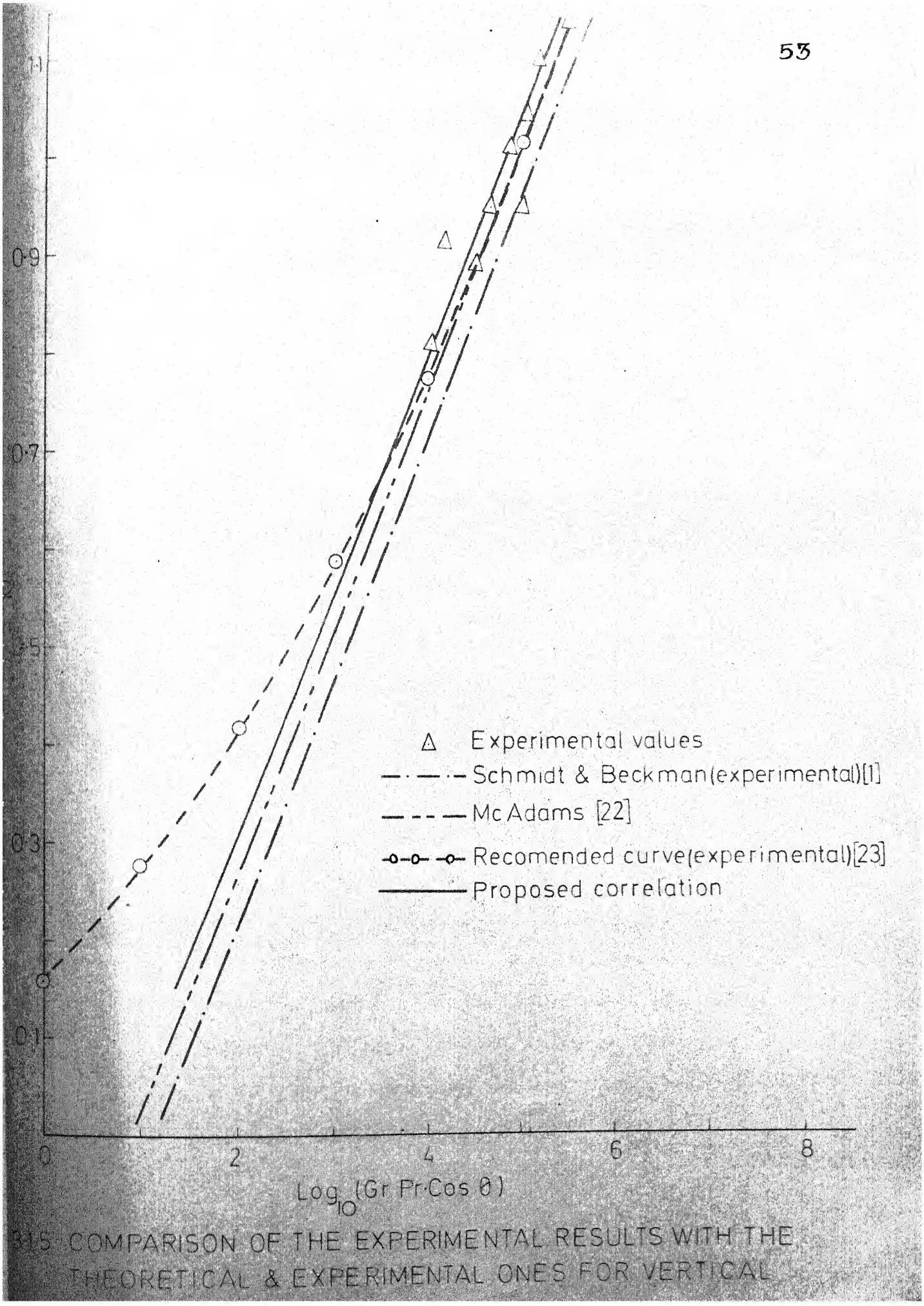

3.5 COMPARISON OF THE EXPERIMENTAL RESULTS WITH THE THEORETICAL & EXPERIMENTAL ONES FOR VERTICAL

yielded by the proposed correlation are, however, seen to be 6.6% and 20.6% higher than those of McAdams [22] and Schmidt & Beckman [1] respectively. The recommended curve of Saunders [23] for short vertical plates, also compares well with the proposed correlation for the range of Grashof numbers experimentally obtained in the present study.

As mentioned earlier, the higher heat transfer coefficients obtained in the present investigation could be explained by the fact that the flow was not restricted to a 2-dimensional configuration, since the plate was open to flow from all sides.

3.2 CONCLUSIONS :

(1) Natural convection heat transfer from an inclined flat plate facing downwards can be evaluated by using the correlation

$$Nu = 0.626\ (Gr.\ Pr.\ Cos\theta)^{1/4}$$

(2) The average heat transfer coefficients yielded by the above proposed correlation are 6.6% higher than McAdam's [22] correlation for vertical plates. This discrepancy is believed to be as a result of the edge effects of the assembly. The boundary layer development on all the edges helps to augment the main flow from the surface of the plate and therefore, results in higher heat transfer coefficients at the edges of the plate. This view was

further confirmed by examining the test plate on the Schlieren bench for flow visualization.

(3) For the horizontal plate facing downwards the average heat transfer coefficient can be obtained from the equation

$$Nu = c\ (Gr.\ Pr.)^{1/5}$$

where the value of c for the present rectangular test plate with free edges was found to be 0.753. The average heat transfer for the horizontal flat plate with free edges and facing downwards are approximately 6% higher than those for 2-dimensional flow experiments reported by Aihara, et. al. [15] .

(4) For the horizontal flat plate facing downwards the boundary layer is seen to be maximum near the center which reduces gradually to the minimum around the free edges. The vertical plume near the edges is observed to accelerate the flow and thereby result in local heat transfer coefficients higher at the edges compared to those at the center of the plate.

3.3 SCOPE FOR FUTURE WORK :

Since the experimental results from the above study cover only a small range of Grashof numbers between 10^4 to 10^5, the scope

of the present study is limited. It is therefore, essential and desirable to extend the range of application of the above proposed correlation to include large Grashof numbers. This would also enable one to find the critical Grashof number at which the breakdown of the laminar flow occurs.

Special provisions are, however, necessary to obtain such large Grashof numbers in stationary apparatus. Grashof number for free convection under the influence of gravitational force g is given by

$$Gr = \frac{g L^3 \beta (t_w - t_a)}{\nu^2}$$

A high Grashof number can be obtained in an experimental set up by having a fluid with a large β/ν^2 ratio, or by making the characteristic dimension, L , sufficiently long or still further by maintaining a large temperature difference between the plate surface and the surroundings. For air at 122F° and 14.22 psia, $\beta = 1.72 \times 10^{-3}$ R°-1, $\nu = 19.89$ ft^2/sec., and $\beta/\nu^2 = 0.434 \times 10^5$. For water at 212F°, (Saturated state) $\beta/\nu^2 = 351 \times 10^5$. Water has β/ν^2 ratio which increases with temperature. However, temperature in an experimental set up would have to be kept well below 212F° to avoid evaporation, in the absence of any pressurization of the equipment.

Gases generally have lower values of β/ν^2 than liquids; however, the ratio β/ν^2 can be increased for gases by increasing the pressure in the system.

REFERENCES

1. SCHMIDT, E, and W.BECKMAN, Boundary-Layer Theory, SCHLICHTING,H; McGraw-Hill, New York, 1968, p.302.

2. ECKERT, E.R.G, and T.W. JACKSON, Analysis of Turbulent Free - Convection Boundary Layer on a Flat Plate, NACA rep. 1015, 1951.

3. ECKERT, E.R.G, and E. SOEHNGHEN, Proceedings of the General Discussion on Heat Transfer, ASME, New York, 1951, p. 321-323, 387-388.

4. OSTRACH, S; An Analysis of Laminar Free-Convection Flow and Heat Transfer about a Flat Plate Parallel to the Direction of the Generating Body Force, NACA TR. 1111, 1953.

5. ECKERT, E.R.G, and A.J. DIAGVILLA, Experimental Investigation of Free-Convection Heat Transfer in a Vertical Tube at Large Grashof number, NACA Rep. 1211, 1955.

6. LIETZKE, A.F; Theoretical and Experimental Investigation of Heat Transfer by Laminar Natural Convection between Parallel Plates, NACA Rep. 1223, 1955.

7. GRIFFITHS, E, and A.H. DAVIS; Food Investigation Board, Spec. Rep. 9, Department of Scientific and Industrial Research, H.M. Stationery Office, London, 1922.

8. LEVY, S; Integral Methods in Natural Convection Flow, J. Applied Mechanic, Vol. 22, 1955, p. 320.

9. WAGNER, C; Discussion - Integral Method in Natural Convection Flow, Journal of Applied Mechanic, Vol. 23, 1956, p. 320.

10. STEWARTSON, K; On the Free Convection from a Horizontal Plate, ZAMP, Vol. 9, 1958, p. 276.

11. KADAMBI, V; Free Convection Heat Transfer from a Horizontal Circular Plate, Master of Science Thesis, Princeton University 1959.

12. KADAMBI, V. and DRAKE, R.M; Free Convection Heat Transfer from Horizontal Surfaces for Prescribed Variation in Surface Temperature and Mass Flow through the Surface, Tech. Report MECH. Eng. HT - 1, Princeton University, 30th June 1960.

13. SINGH, S.N; R.C. BIRKEBAK and R.M. DRAKE, Jr; Laminar Free Convection Heat Transfer From Downward Facing Horizontal Surfaces of Finite Dimensions, Progress in Heat & Mass Transfer, Vol. 2, p. 87, Pergaman Press Oxford, 1969.

14. CLIFTON, J.V; and CHAPMAN, A.J; Natural Convection on a Finite Size Horizontal Plate, Int. J. Heat & Mass Transfer, Vol. 12, 1969, pp. 1573-1584.

15. AIHARA, T; YAMADA, Y. and ENDŌ, S; Free Convection along the Downward Facing Surface of a Heated Horizontal Plate, Int. J. Heat and Mass Transfer, Vol. 15, 1972, pp. 2535-2549.

16. FRANCISCO and GLICKSMAN; The Effect of Edge Condition on Natural Convection from a Horizontal Plate, Int. J. Heat and Mass Transfer, Vol. 17, 1974, p. 135.

17. RICH, B.R; An Investigation of Heat Transfer From an Inclined Plate in Free Convection, TRANS. ASME, Vol. 75, 1953, p. 489.

18. VLIET, G.C; Natural Convection, Local Heat Transfer on Constant Heat Flux Inclined Surface, Trans. Am. Soc. Mech. Engrs. Vol. 91C, 1969, pp. 511-516.

19. International Critical Tables, Vol. 5, p. 234, New York, McGraw-Hill Book Co; 1929.

20. LORENTZ, The Theory of Electrons, p. 145, 1909.

21. KOTHANDARAMAN and SUBRAMANYAN; Heat and Mass Transfer Data Book, Wiley Eastern, Pvt. Ltd. India, Sec. Ed; p. 20.

22. McAdams, W.H; Heat Transmission, 3rd. Ed. McGraw-Hill, New York, 1954, p. 172.

23. Saunders, O.A; Proc. Roy. Soc (London), Vol. A 157, 1936, pp. 278-291.

15. AIHARA, T; YAMADA, Y. and ENDŌ, S; Free Convection along the Downward Facing Surface of a Heated Horizontal Plate, Int. J. Heat and Mass Transfer, Vol. 15, 1972, pp. 2535-2549.

16. FRANCISCO and GLICKSMAN; The Effect of Edge Condition on Natural Convection from a Horizontal Plate, Int. J. Heat and Mass Transfer, Vol. 17, 1974, p. 135.

17. RICH, B.R; An Investigation of Heat Transfer From an Inclined Plate in Free Convection, TRANS. ASME, Vol. 75, 1953, p. 489.

18. VLIET, G.C; Natural Convection, Local Heat Transfer on Constant Heat Flux Inclined Surface, Trans. Am. Soc. Mech. Engrs. Vol. 91C, 1969, pp. 511-516.

19. International Critical Tables, Vol. 5, p. 234, New York, McGraw-Hill Book Co; 1929.

20. LORENTZ, The Theory of Electrons, p. 145, 1909.

21. KOTHANDARAMAN and SUBRAMANYAN; Heat and Mass Transfer Data Book, Wiley Eastern, Pvt. Ltd. India, Sec. Ed; p. 20.

22. McAdams, W.H; Heat Transmission, 3rd. Ed. McGraw-Hill, New York, 1954, p. 172.

23. Saunders, O.A; Proc. Roy. Soc (London), Vol. A 157, 1936, pp. 278-291.

APPENDIX - A

THERMOCOUPLE CALIBRATION

Thermocouple is an important, accurate and stable temperature measuring device with rapid response and low maintenance cost. It consists of two dissimilar electrical conductors either or both of which may be pure metals, alloys or non - metals, having a common junction where the conductors are in good thermal and electrical contact. Common type of thermocouples are Copper - constantan, Iron - constantan, Chromel - alumel etc. and their selection for a particular use depends upon various factors like range of temperature measurements needed and the type of atmosphere surrounding the measuring junction. For the present work, Chromel - alumel Thermocouples have been chosen.

Measurement of temperature by means of thermocouple is based on the simple fact that when two junctions formed by two dissimilar conductors are maintained at different temperatures, a small electromotive force is generated in the circuit, the magnitude of which depends upon the temperature difference between the junctions. Every thermocouple bears a certain relationship between the temperature difference of the two junctions and electromotive force generated in the circuit.

The simplest thermocouple circuit arrangement is shown in Fig. A-1. One of the junctions called cold junction (or reference junction) is maintained at fixed known temperature (usually at ice point), and the other junction known as hot junction is inserted at the unknown temperature bath. The thermocouple may be lengthened, to remove the effective cold junction from the influence of heated zone either by adding compensating leads made from materials identical to those of the thermocouple or by forming a thermocouple pair of similar emf characteristics over the range of temperatures to which the ends of the compensating leads are likely to be exposed. A sensitive and accurate millivolt potentiometer may be used to measure the emf generated in the circuit and by using the relationship between the temperature difference between the two junctions and the emf developed in a particular thermocouple, the unknown temperature is calculated.

The temperature-emf relationship of a thermocouple depends upon the type of metals used. (In the manufacture of thermocouples it is inevitable that some impurities will be present in quite appreciable proportions). Moreover, this relationship depends upon the way in which the junctions are made and the type of lead wires used for connecting the thermocouples to the emf measuring device. Therefore, whenever high accuracy is desired, proper calibration of the thermocouple is necessary. In the present work, the thermocouple was calibrated against a standard Platinum Resistance Thermometer (Leeds and Northrup Company).

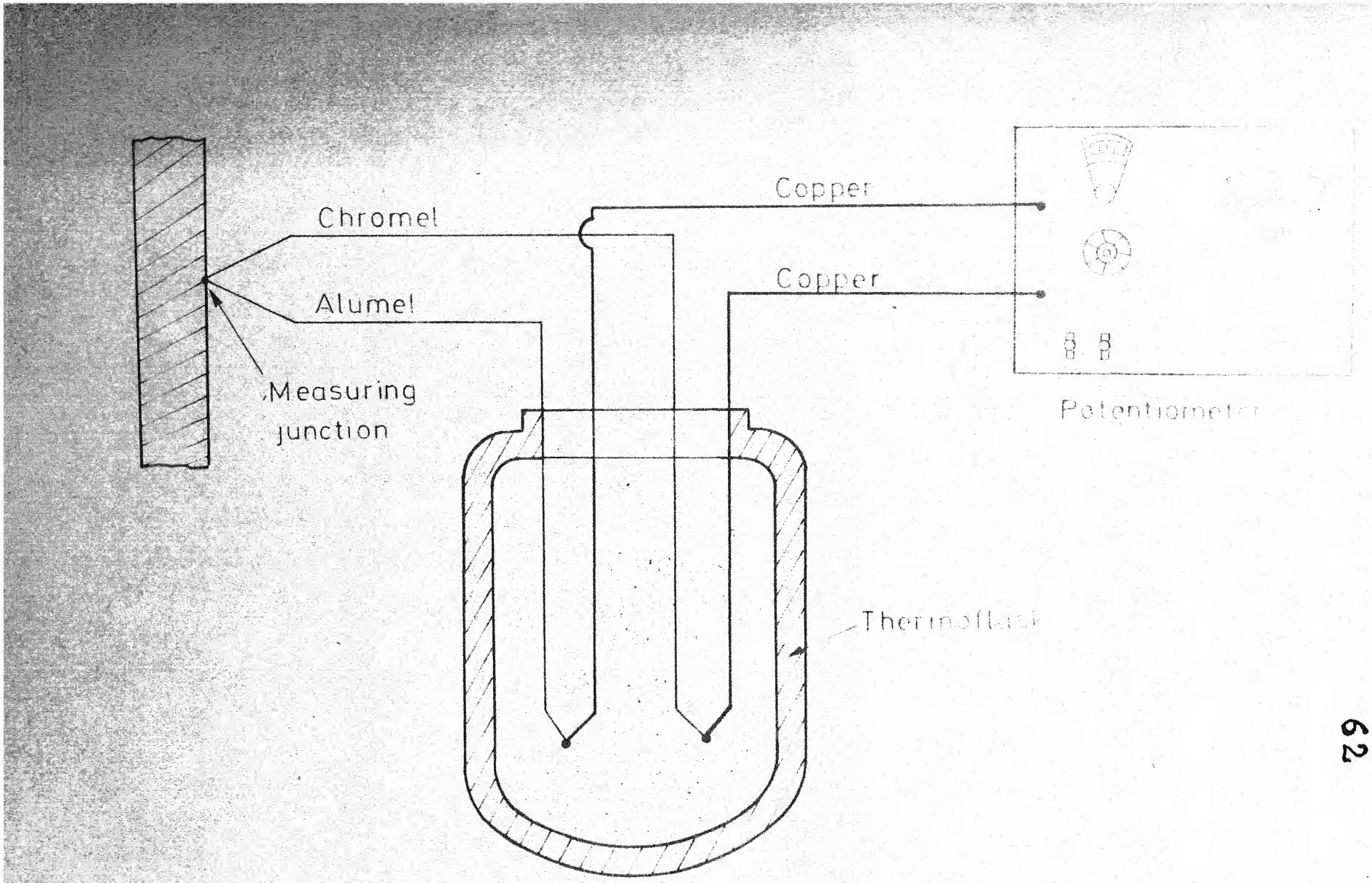

FIG A-1 THERMOCOUPLE CIRCUIT

A Muller's bridge, also of the Leeds and Northrup Company was used to measure the resistance of the platinum resistance thermometer. The resistance of this thermometer bears a certain relationship with the temperature surrounding the element of platinum resistance thermometer. This relationship is in the form of charts and mathematical formulae supplied with the thermometer.

The emf generated in the circuit has been measured by the potentiometer (Leeds and Northrup) with least count 0.005 mV. Potentiometers have advantage over the other types of emf measuring devices in the fact that they draw no current from the source of unknown voltage when the circuit is balanced for emf measurement. The unknown voltage is balanced against a known potential drop which is due to the flow of current through some standard resistances.

Muller's bridge is nothing but an improvement of the basic Wheatstone bridge to facilitate very accurate resistance measurements. The one used in the present work is that of Leeds and Northrup Company and has one high resistance range and three low resistance ranges. The latter has again three resistance measuring ranges enabling it to be used with thermometers having low (0.25 - 1.00 ohm), intermediate (10 - 100 ohms) or high (greater than 1,000 ohms) resistance values at 0 °C. In the intermediate range resistance values are exactly reproducible to the fourth decimal place. The platinum resistance thermometer used

in the present work has a reported resistance of 25.554216 Ohms at 0 °c. So the intermediate range is chosen for the present work. The Mu ller's bridge has a built-in galvanometer for null detection when the circuit is balanced. But this needs a Battery of 8.48 volts exact. Since the battery to this requirement was not available, an external Leeds and Northrup galvanometer was used with the bridge for null detection.

The Chromel-Alumel thermocouples used in the present work have been calibrated against the platinum resistance thermometer in a constant temperature vapour bath. The schematic diagram of this set-up is given in Fig. A-2. The main part of this apparatus is the Vapour Jacket 'VJ' which is connected to the side arm flask in which a pure liquid (say bromo-benzene) is taken and boiled at a constant total pressure in an inert atmosphere of nitrogen. The vapours will rise through the jacket to the condenser CD where they will be condensed and circulated back to the side arm flask. As it is known that the pure liquid boils at a constant temperature when the total pressure is fixed, by maintaining different total pressures inside the jacket with the help of nitrogen, different constant temperatures can be maintained inside the jacket with a single pure substance. In order to damp out the pressure fluctuations and thereby temperature fluctuations, the volume of the system was increased by connecting two 20 - liter flasks (Ballasts) to the system. Changes in the nitrogen pressure of the system can be

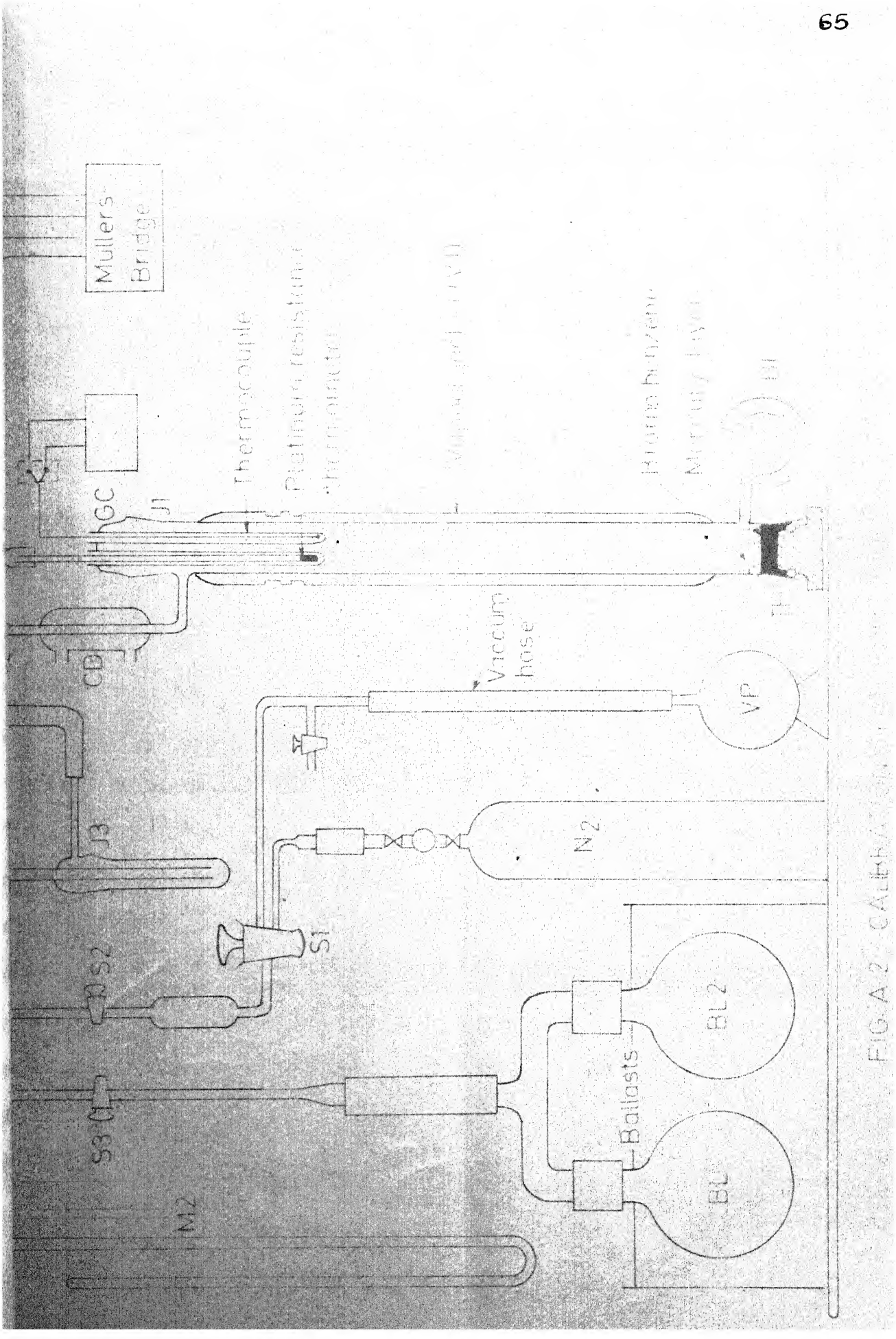

FIG A.2 CALIBRATION

affected by the vacuum pump 'VP' and high pressure nitrogen cylinder with a low pressure regulator connected to the system. The vapour jacket has a glass cap at the top which carries two thermowells in the vapour jacket. One of the wells receives the platinum resistance thermometer with 7" depth of immersion as calibrated by the U.S. National Bureau of Standards. The hot junction of thermocouple is inserted into the other well upto the same depth. In both the wells Silicone Oil is filled (between one and two inches depth), to ensure good thermal contact. The bottom of the vapour jacket is plugged by means of a Teflon plug with an O - ring outside. Mercury is poured onto this plug so as to keep O ring away from chemical used in the jacket and also to prevent any leakage through this joint. Bromobenzene has been used for calibration upto 160 °C.

To maintain the cold junction of thermocouple at ice point an equilibrium solution of crushed ice and distilled water was taken into a thermoflask. Ice is added from time to time and ice and water slurry is stirred thoroughly with glass rod in order to ensure its solution temperature at 0 °C. An accurate thermometer is also inserted into this bath to check the constancy of temperature inside it.

The resistance - temperature relationship for the platinum resistance thermometer is given by the Callender's Equation as:

$$t' = \frac{100\,(R_{t'} - R_o)}{R_{100} - R_o} + \delta\left(\frac{t'}{100} - 1\right)\frac{t'}{100}$$

$$= \frac{1}{\alpha}\left(\frac{R_{t'}}{R_o} - 1\right) + \delta\left(\frac{t'}{100} - 1\right)\left(\frac{t'}{100}\right)$$

An alternative form of the above can be written as

$$R_{t'} = R_o\,(1 + a\,t' + b\,t'^2)$$

where

$$a = \alpha(1 + \delta/100)$$

$$b = -\frac{\alpha\delta}{10^4}$$

The reported values of the constants by U.S. Bureau of Standards are given below :

R_o (Resistance at ice point) = 25.5814 Ohms.

α (Fundamental coefficient of coil) = 0.003926833

δ = 1.496176

R_o has been checked for the ice point with Muller's bridge and found in good agreement with the reported value within $\pm$ 0.0001 Ohm. Using the above formula and constants, a table has been generated with the help of the computer to give the resistance value of thermometer at 0.005 °C temperature intervals from 0 °C to 300 °C. This table can be used directly to read the temperature from the resistance of platinum resistance thermometer. In this way it has been observed that with this kind of apparatus any thermocouple can accurately be calibrated. The calibration curve is shown in Fig. A-3.

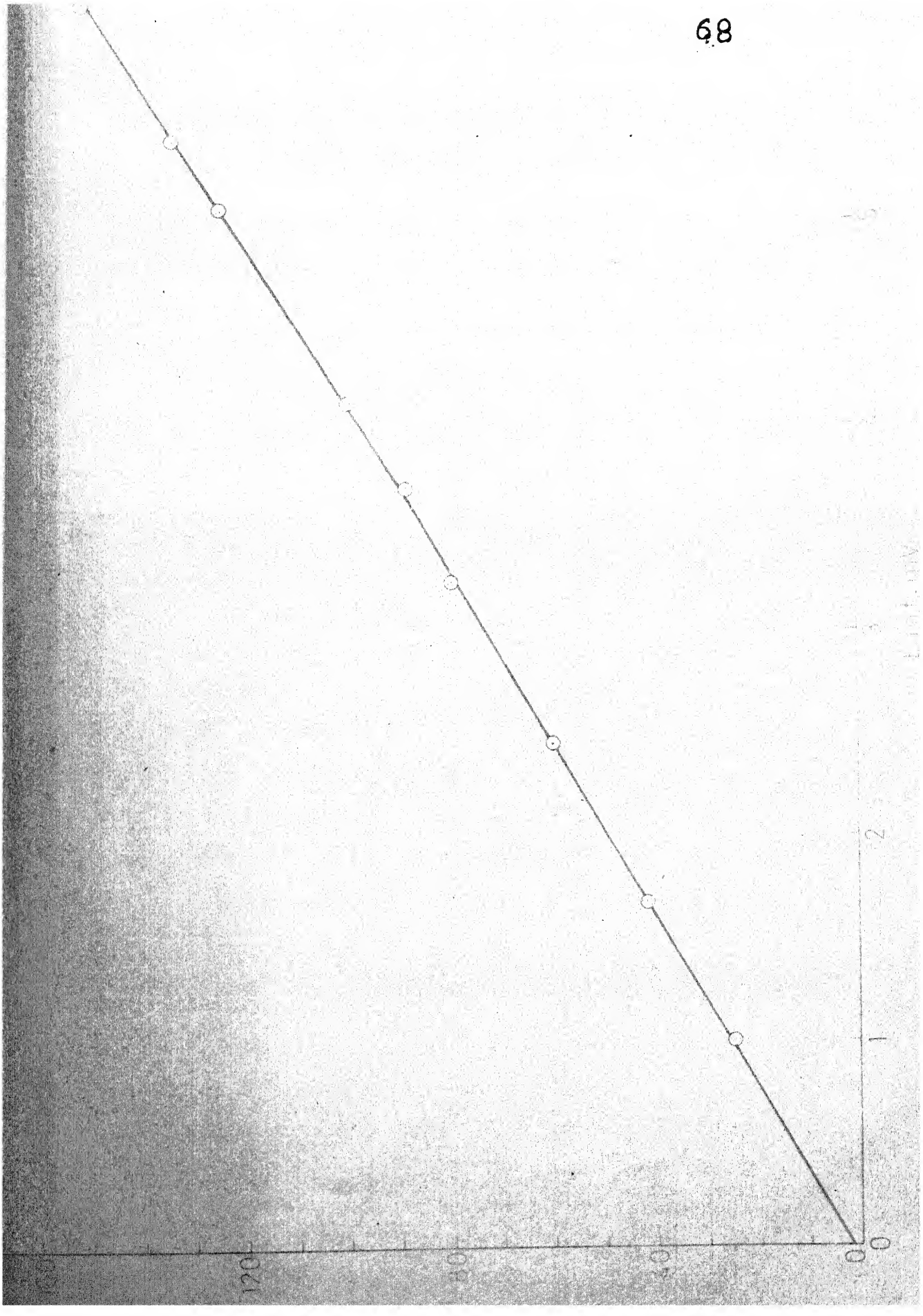
120
0
0

APPENDIX - B

The set of calculations given below applies to the interferogram for the configuration $\theta = 30$, $x/L = 2/3$ and $\triangle t_w = 30.0\ c^o$. The fringe shifts as measured with an optical projector are tabulated as below :

S(mm)	0	1	2	3	4	5
$\triangle N$	4.5	3.6	2.7	1.8	1.0	0.6
$\triangle T(K^o)$	30.0	23.4	17.5	11.8	6.6	3.8

Ambient temperature, $t_a = 29.5\ c^o$

Length of the path of light, $l = 120$ mm

Wave length of He-Ne laser light

in vacuum, $\lambda_o = 63.28 \times 10^{-5}$ mm

$(n_a - 1)$ from Ref. [19] $= 26.247 \times 10^{-5}$

when S = 0 i.e. at the plate surface itself using equation (9) sec. 2.5, we have

$$\triangle T = T_a \frac{\triangle N}{(n_a - 1)\frac{1}{\lambda_o} - \triangle N}$$

$$= (273 + 29.5) \times \frac{4.5}{\frac{26.247 \times 10^{-5} \times 120}{63.28 \times 10^{-5}} - 4.5}$$

$$= \frac{302.5 \times 4.5}{49.75 - 4.5}$$

$$= 30.0 \text{ K}^\circ$$

similarly, $\triangle T$ was calculated for other distances from the plate and the values entered into the above table. The temperature distributions as calculated from the interferogram is shown in Fig. 3.1.3. From this figure, the temperature gradient at the wall is

$$\frac{dT}{ds} = -63.1 \text{ c}^\circ/\text{cm}$$

Wall heat flux $q_w = h_x(t_w - t_a) = -k\frac{dT}{ds}$

$$h_x = -\frac{k}{t_w - t_a} \cdot \frac{dT}{ds}$$

$$Nu_x = \frac{h_x x}{k} = -\frac{x}{t_w - t_a} \cdot \frac{dT}{ds}$$

$$= \frac{4}{30.0} \times 63.1 = \underline{8.42}$$

Wall temperature $t_w = 29.5 + 30.0 = 59.5 \text{ c}^\circ$

Mean film temperature $t_f = \frac{t_w + t_a}{2} = \frac{59.5 + 29.5}{2}$

$$= 44.5 \text{ c}^\circ$$

Property values for air Ref. [21] at 44.5 c° and one standard atmospheric pressure are as follows:

$K = 24.0 \times 10^{-5}$ Kcal/hr-cm-c°

$\nu = 0.1745$ cm^2/sec.

$Pr = 0.6985$

Since air at atmospheric pressure can be treated as an ideal gas, the coefficient of thermal expansion, β, is the reciprocal of the absolute temperature.

Thus, $$Gr_x = \frac{981 \times (4)^3 \times 30.0}{(0.1745)^2 \times 302.5} = \underline{1.885 \times 10^5}$$

$$(Gr\ Pr\ Cos\theta)_x = (1.885 \times 0.6985 \times Cos\ 30)10^5$$

$$= 1.14 \times 10^5$$

$$(Gr\ Pr\ Cos\theta)_x^{\frac{1}{4}} = (11.4)^{\frac{1}{4}} \times 10 = \underline{18.35}$$

$$c_x = \frac{Nu_x}{(Gr\ Pr\ Cos\theta)_x^{\frac{1}{4}}} = \underline{0.458}$$